Supplementary Information

Bi-Ligands Fabricated CdS Quantum Dots to Photo-induce Aqueous-Phase Aldol Condensation for Biomass-derived Carbonyl Compounds

Dong-Dong Wei, Liu-Meng Mo, Jing-Yu Zhang, Yong-Shuai Zhang, Hui-Min Duan, Bin Zhang, Hong-Yan Wang*

Key Laboratory for macromolecular Science of Shaanxi Province, School of Chemistry and Chemical Engineering, Shaanxi Normal University, Xi'an, 710119, China

*Correspondence E-mail: hongyan-wang@snnu.edu.cn

Table of Contents

1. Experimental Section

1.1 Materials

All reactions were carried out under an atmosphere of nitrogen, unless otherwise specified. DMPO (dimethyl-1-pyrroline-N-oxide) used for EPR analysis was obtained from Dongren Chemical Technology Co., Ltd., while all other chemicals used in this work were purchased from Energy Chemical Co., Ltd. The purification of the crude reaction products was realized by using thin layer chromatography (TLC) with 300-400 mesh silica gels.

1.2 Characterizations

High-resolution transmission electron microscopy (HR-TEM) images were obtained by using a Tecnai G2 F20 electron microscope operating at 200 kV. An X-ray powder diffractometer (XRD) was operated to characterize the structures of materials on Bruker D8 Advance. X-ray photoelectron spectroscopy (XPS) was performed using the KRATOS Axis ultra DLD X-ray photoelectron spectrometer. UV-vis diffuse reflectance spectrum (UV-vis DRS) was obtained by using a UV-vis-NIR spectrometer (Perkin-Elmer, USA) at room temperature from 200 to 800 nm with $BaSO_4$ pellets as a background. UV-vis absorption spectrum was recorded on U-3900 UV-vis spectrophotometer (Hitachi). Photoluminescent (PL) spectrum was recorded using a fluorescence spectrometer (F-7000, Hitachi). Fourier transform infrared (FT-IR) spectrum was collected on a FT-IR spectrometer (Spectrum One, Perkin Elmer). Electron paramagnetic resonance (EPR) analysis was made by using German Bruker EMX-10/12 electronic paramagnetic spectrometer. Liquid product was

detected on GC MS-QP2010 UItra gas chromatograph with the extracted sample vaporized on the instrument. Pure organic complexes were used as standards to obtain the retention time and to quantify the yields of the reaction products. NMR data (^{1}H NMR and ^{13}C NMR) were recorded with a 400 MHz Brüker spectrometer, in which chemical shift was expressed in parts per million (ppm) unit with tetramethylsilane as the standard. H_2 detection and quantification were carried out using a TCD detection port on TIAN MEI 7900 GC gas chromatograph.

1.3 Synthesis of photocatalysts

1.3.1 The synthesis of CdS-MUA&P

The synthesis of **CdS-MUA&P** was based on a modified procedure recently reported by us.[1] Under a N_2 atmosphere, $CdCl_2 \cdot H_2O$ (114.8 mg, 0.57 mmol) was dissolved in 100 mL of H_2O. To this solution, proline (345.39 mg, 3 mmol) was added, and followed by the addition of 11-mercaptoundecanoic acid (MUA, 109.18 mg, 0.5 mmol). The pH of resulted solution was then adjusted to pH 7 with 1 M NaOH. Upon the reaction, the solution changed from colorless to turbid white, which eventually afforded a colorless transparent solution under successive stirring. After adding 5 mL of 0.1 M Na_2S solution and refluxing the mixture for 4 h, a clear bright orange solution was obtained, which was then evaporated under vacuum to remove the solvent, yielding a yellow viscous liquid. The resulted residue was treated with isopropanol and centrifuged to isolate the unreacted regents. Repeated the above purification twice, which afforded 163 mg **CdS-MUA&P** as light-orange powders after drying under room conditions. Noted that the ratio of MUA and proline can

affect the transparence of reaction system for the synthesis of **CdS-MUA&P** and even the efficiency for photocatalytic aldol condensation. Therefore, the ratio was regulated, which indicated 1: 6 was the best, which not only guaranteed the reaction system transparence for **CdS-MUA&P** synthesis, but also enabled to obtain the highest efficiency for aldol condensation by **CdS-MUA&P**.

1.3.2 The synthesis of CdS-P

The synthesis of **CdS-P** followed the similar method applied for **CdS-MUA&P**, excepted that only proline was added. In typical procedures, 101 mg **CdS-P** was obtianed as yellow powders.

1.3.3 The synthesis of CdS-MUA&P'

The similar procedure with the synthesis of **CdS-MUA&P** was also operated for **CdS-MUA&P'** with N-methyl-proline used instead. In typical procedures, 152 mg **CdS-MUA&P'** was obtained as orange powders.

1.4 The preparation of photocatalytic systems

The photocatalytic aldol condensation was carried out in a quartz test tube under successive stirring at room temperature. In a typical experiment, 5 mg photocatalyst was dispersed in 0.5 mL H_2O. TEA (4 mmol) was then added. The reagent FF or HMF (0.5 mmol) was injected in above reaction system, and then mixed with 1.5 mL biomass-derived ketones, which acted as both substrate and solvent. The total reaction system was 2.5 mL. After purged with N_2 for 30 min, the system was sealed and irradiated with a LED (λ = 420 nm, the input optical power is 8.37 mW cm^{-2}) for 1.5 h. After the photocatalytic reaction, the photocatalytic system was extracted by

CH_2Cl_2 for three times. The organic phase was dried by anhydrous Na_2SO_4 and was evaporated under vacuum. The crude products were further purified using TLC with 300-400 mesh silica gels by the proper elutes. The conversion and yield for the generation of target products were defined as follows:[2]

Conversion (%) = $[(C_0 - C_r)/C_0] \times 100$

Yield (%) = $C_p / C_0 \times 100$

in which C_0 is the initial concentration of reactant, C_r and C_p are the concentrations of reactant and target products at a certain reaction time, respectively.

2. Supporting Figures and Tables

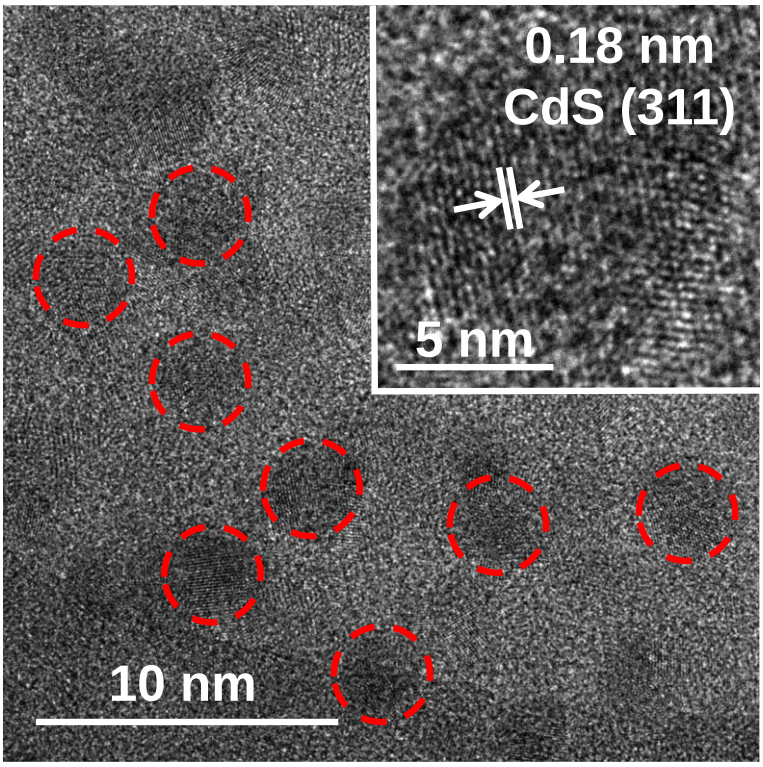

Fig. S1 The HR-TEM image of **CdS-MUA&P**.

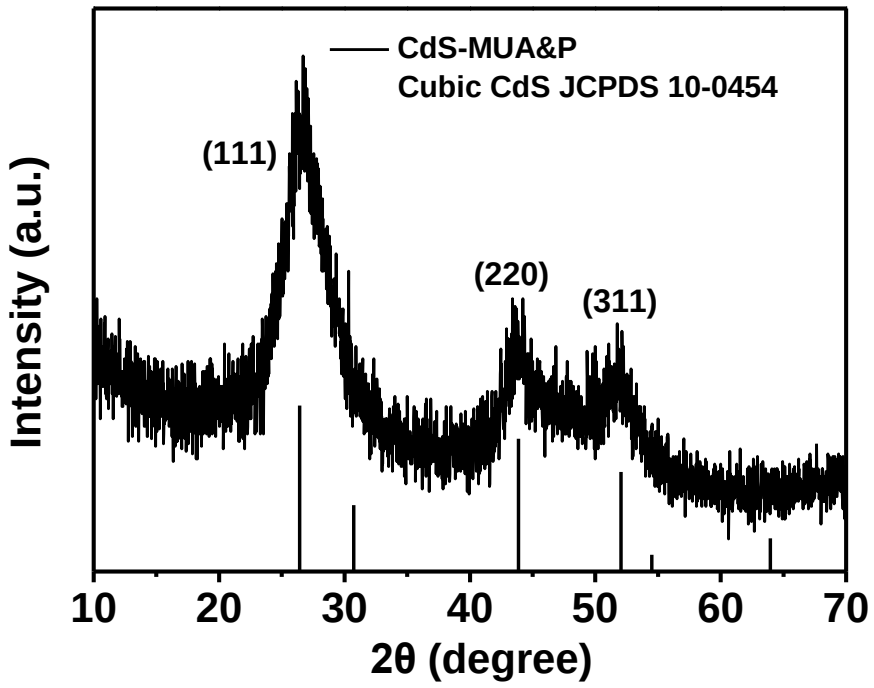

Fig. S2 The XRD spectrum of **CdS-MUA&P**, showing characteristic CdS peaks (JCPDS 10-0454): the 2θ at 26.69°, 43.88° and 51.91° corresponded to the (111), (220) and (311) planes of a cubic structure, respectively.[3]

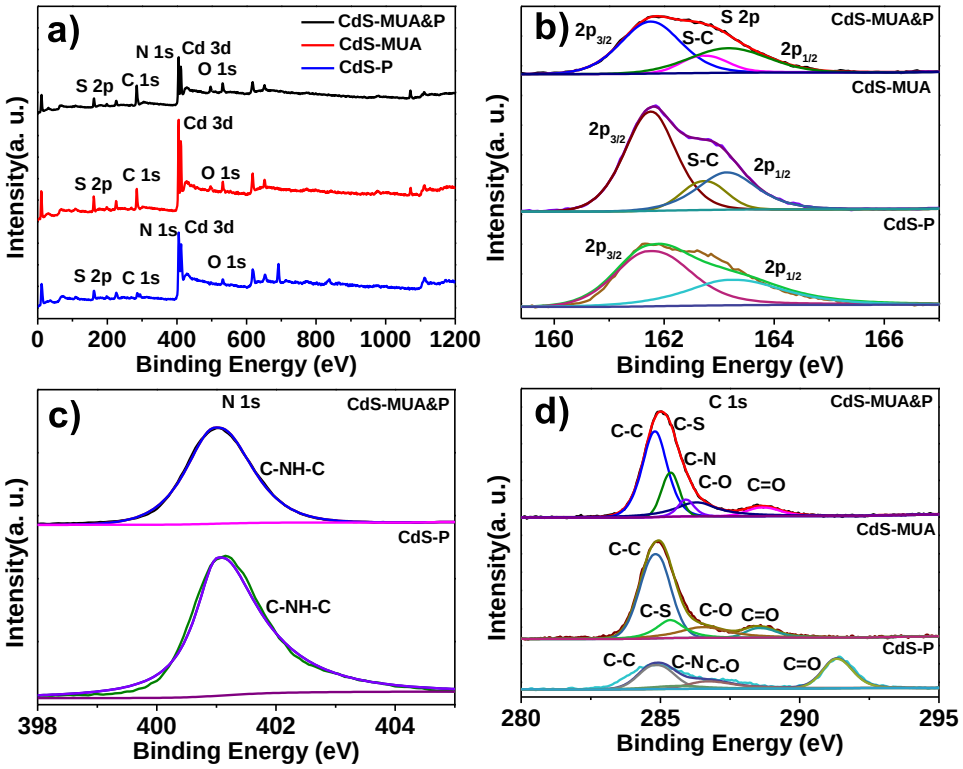

Fig. S3 The XPS spectra of (a) full spectrum, (b) S 2p, (c) N 1s, (d) C 1s for **CdS-MUA&P**, **CdS-MUA** and **CdS-P** respectively.

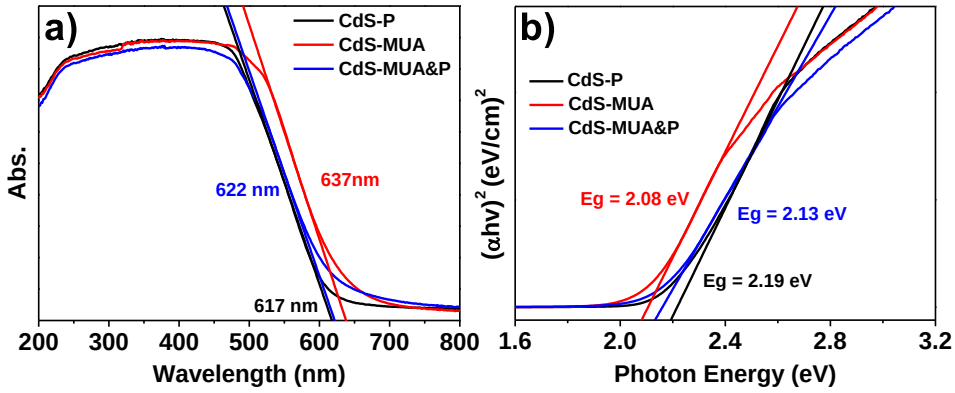

Fig. S4 a) The UV-vis DRS spectra of **CdS-P**, **CdS-MUA**, **CdS-MUA&P** respectively; b) the corresponding Tauc plots $(ahv)^2$ plots versus hv for each material.

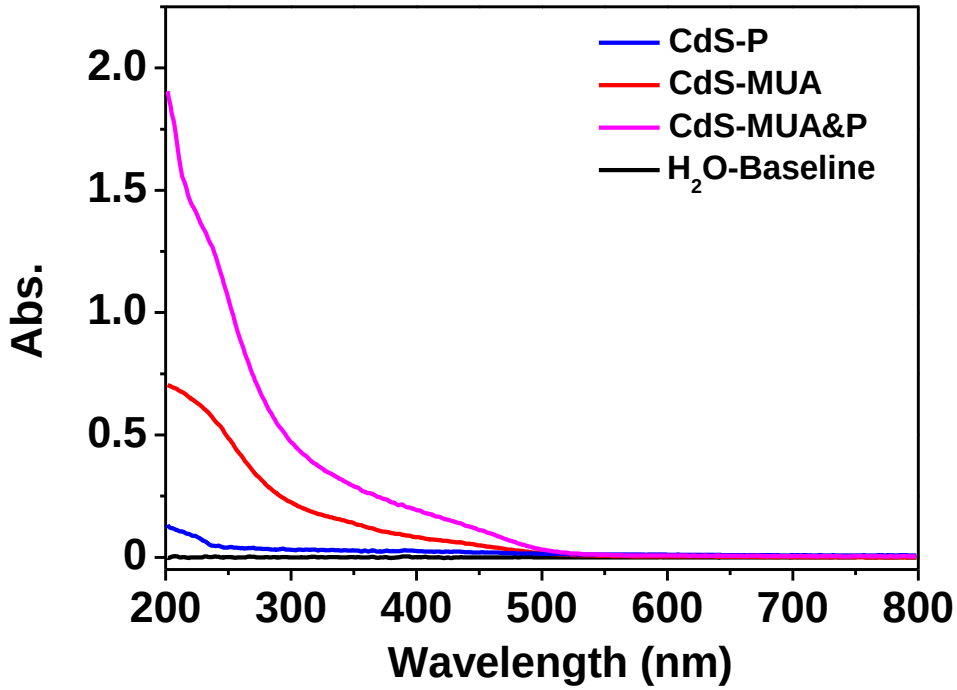

Fig. S5 UV-vis spectrum of **CdS-MUA&P**, **CdS-MUA** and **CdS-P**.

Based on the equations suggested by Peng and coworkers, the diameter (D), extinction coefficient (ε) and concentration (c) of QDs can be determined as follows:[4]

$$D = \left(-6.6521 \times 10^{-8}\right)\lambda^3 + \left(1.9557 \times 10^{-4}\right)\lambda^2 - \left(9.2352 \times 10^{-2}\right)\lambda + (13.29) \quad (1)$$

$$\varepsilon = 21536(D)^{2.3} \quad (2)$$

$$Abs = \varepsilon cL \quad (3)$$

in which D (nm) is the size or diameter of nanocrystal sample, and λ (nm) is the wavelength of its first excitonic absorption peak, ε represents the extinction coefficient of nanocrystal (mol L^{-1} cm^{-1}), L (cm) is cuvette length in the direction of irradiation, Abs is the absorbance of sample and c represents its concentration (mol L^{-1}).

Accordingly, the concentration of **CdS-MUA&P**, **CdS-MUA** and **CdS-P** was evaluated as 2.79 $\times 10^{-5}$, 1.05 $\times 10^{-5}$ and 1.21 $\times 10^{-6}$ mol L^{-1} respectively. Here, we described the concentration

determination process for QDs in water, which facilitated to compare PL under the similar concentration and conditions.

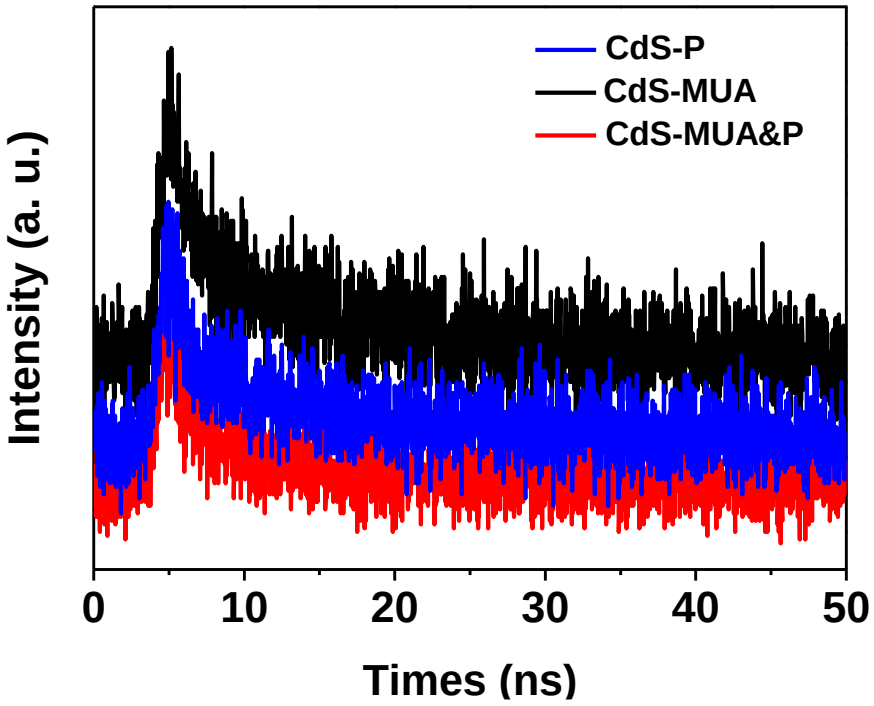

Fig. S6 The time-resolved photoluminescence decay of **CdS-MUA&P, CdS-MUA, CdS-P** respectively**.**

The time-resolved photoluminescence curves were fitted by a biexponential function based on the equation (4):[5]

$$I(t) = A_1 \exp(-t/\tau_1) + A_2 \exp(-t/\tau_2) \quad (4)$$

in which τ_1 and τ_2 represent for the short and long lifetime of decay respectively, and A_1 and A_2 are the amplitudes of photoluminescence. The average lifetime τ was calculated as the equation (5):[5]

$$\tau = \frac{\sum A_i \tau_i^2}{\sum A_i \tau_i} \quad (5)$$

The τ_1, τ_2 and τ for **CdS-MUA&P**, **CdS-MUA** and **CdS-P** were listed in Table S3 respectively.

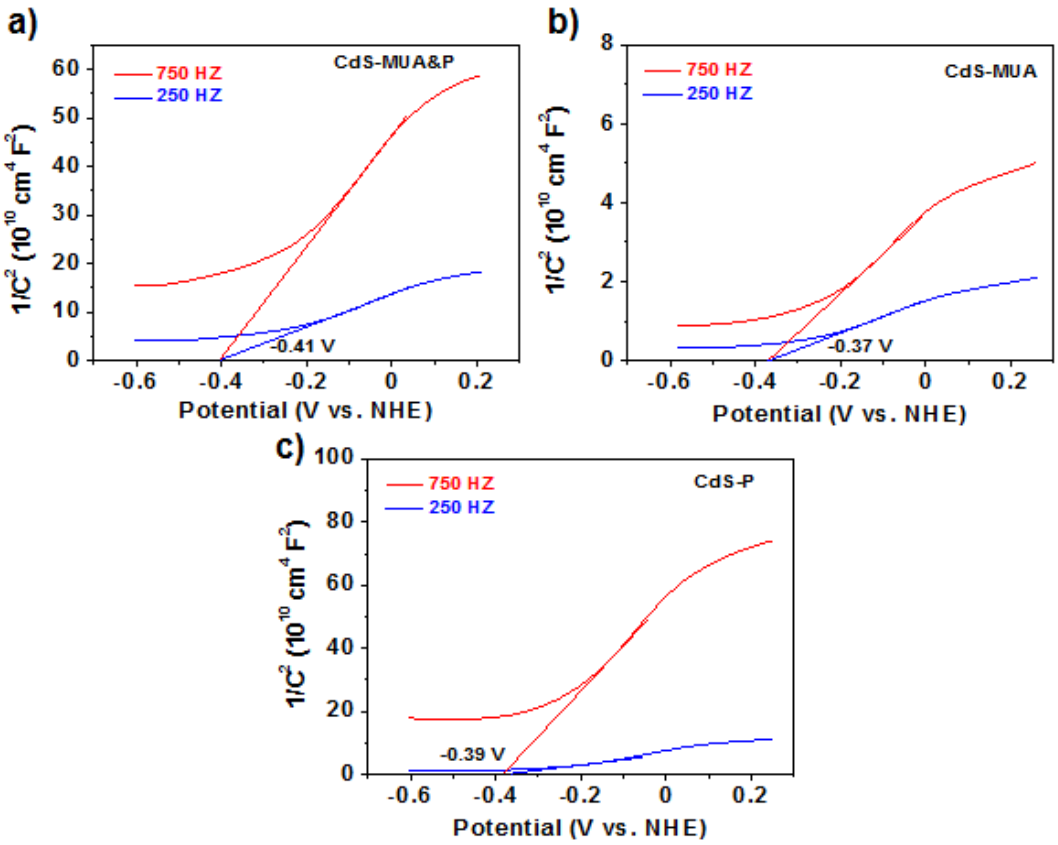

Fig. S7. The Mott-Schottky (MS) curves for determining the band location of each sample.

As a typical n-type semiconductor, CdS OQs have the negligible gap between flat band potential (Vfb) and bottom edge of CB.[6] As shown in Fig. S7, **CdS-MUA&P**, **CdS-MUA** and **CdS-P** displayed the position of CB at -0.41 eV, -0.37 eV and -0.39 eV respectively. Based on the E_g estimated from UV-vis DRS spectra in Fig. S4, the VB were located at 1.72 eV, 1.71 eV and 1.80 eV respectively.

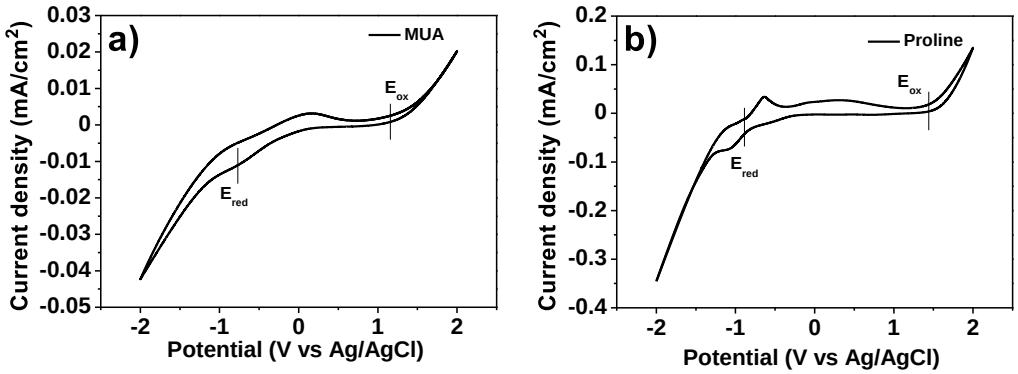

Fig. S8 CV spectra of (a) MUA and (b) proline in CH_3CN respectively, which was carried out with bare FTO electrode as working electrode, Ag/AgCl electrode as reference and graphite rod as a counter electrode with Bu_4NPF_6 as supporting electrolyte.

The determination for the HOMO band level of CDs was based on CV measurement, which was according to the following equation:[7]

$$E_{HOMO} = -(E_{ox} + E_{ref}) \quad (6)$$

Here, E_{ox} represents the first oxidation potential, and E_{ref} is the potential of the reference electrode, in which the potentials were reference to the Ag/AgCl electrode. The values of E_{HOMO} were evaluated versus vacuum level.

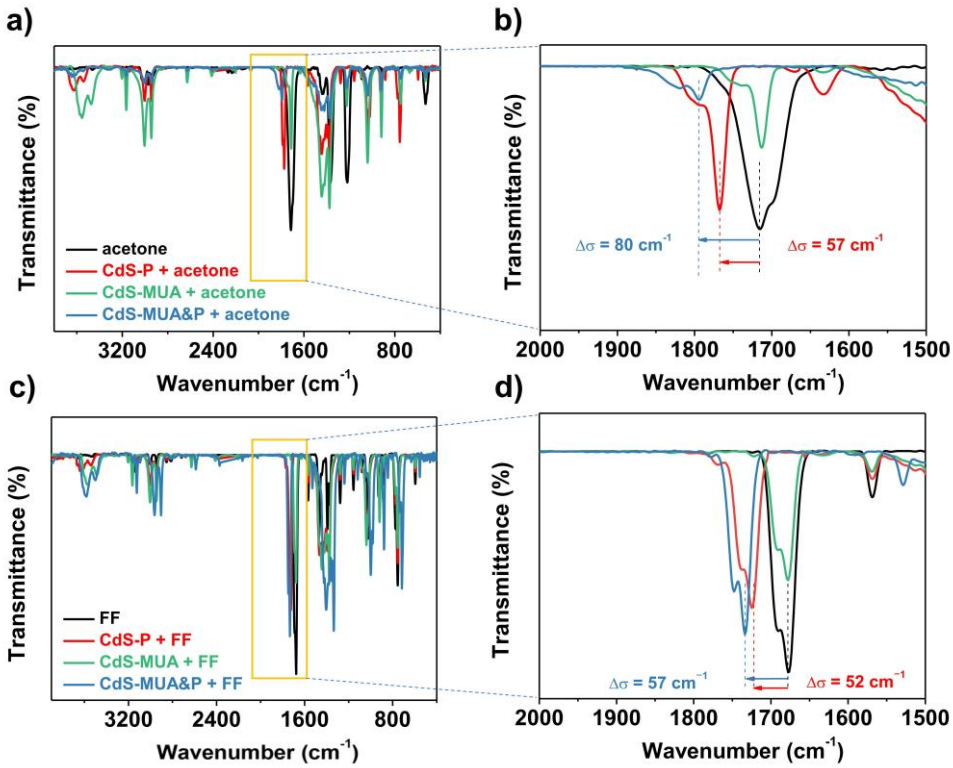

Fig. S9 FT-IR spectra of (a) acetone and (c) FF with different photocatalytic samples or without photocatalytic samples in CH_3CN; (b) and (d) the enlarged spectra in the C=O signal range.

Fig. S9 exhibited the IR spectra of acetone, the mixture of acetone and **CdS-P**, the mixture of acetone and **CdS-MUA**, and the mixture of acetone and **CdS-MUA&P** respectively. Since C=O groups displayed the signal around 1700 cm^{-1}, Fig. S9 (b) showed the enlarged picture in such the signal ranges. It is distinct acetone displayed stretching vibrations of C=O 1715 cm^{-1}, which moved to 1794 cm^{-1} in the mixture of acetone and **CdS-MUA&P**. Such the shift (Δσ) was also observed when **CdS-MUA&P** was switched into **CdS-P** with the shift of 57 cm^{-1}, but absent with **CdS-MUA** applied instead. Similarly, the shift of C=O group on FF was also detected in the mixture of FF and **CdS-MUA&P** or the mixture of FF and **CdS-P**. However, switching into

CdS-MUA, the shift was not observed. These results confirmed that H-bonds were formed between NH moiety on proline of QDs and carbonyl groups on FF and acetone.

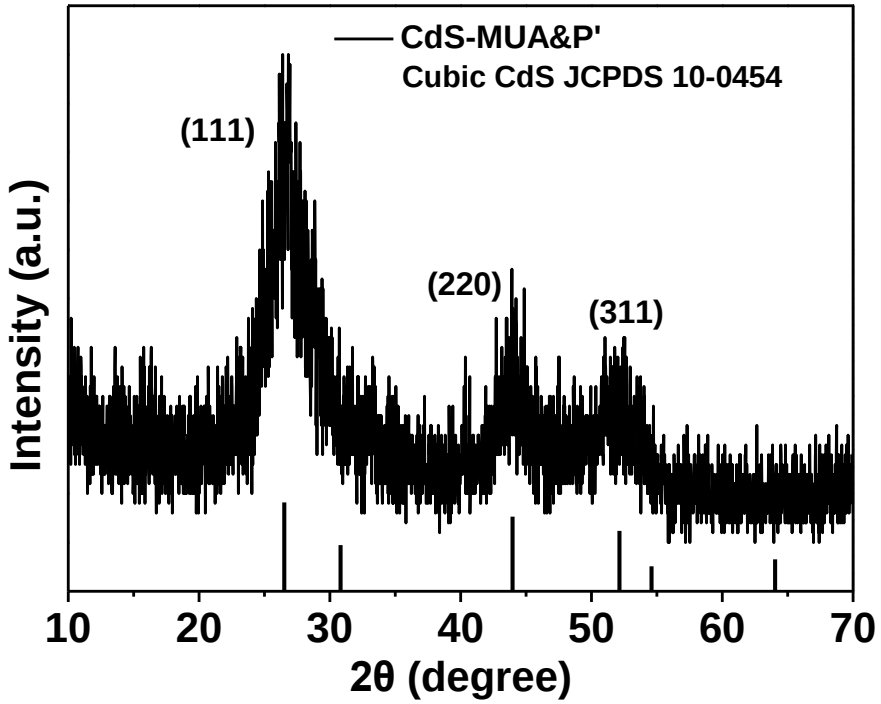

Fig. S10 The XRD spectrum of **CdS-MUA&P'**, showing characteristic CdS peaks (JCPDS 10-0454): the 2θ values of 26.58°, 43.86° and 51.96° corresponded to the (111), (220) and (311) planes of a cubic structure, respectively.[3]

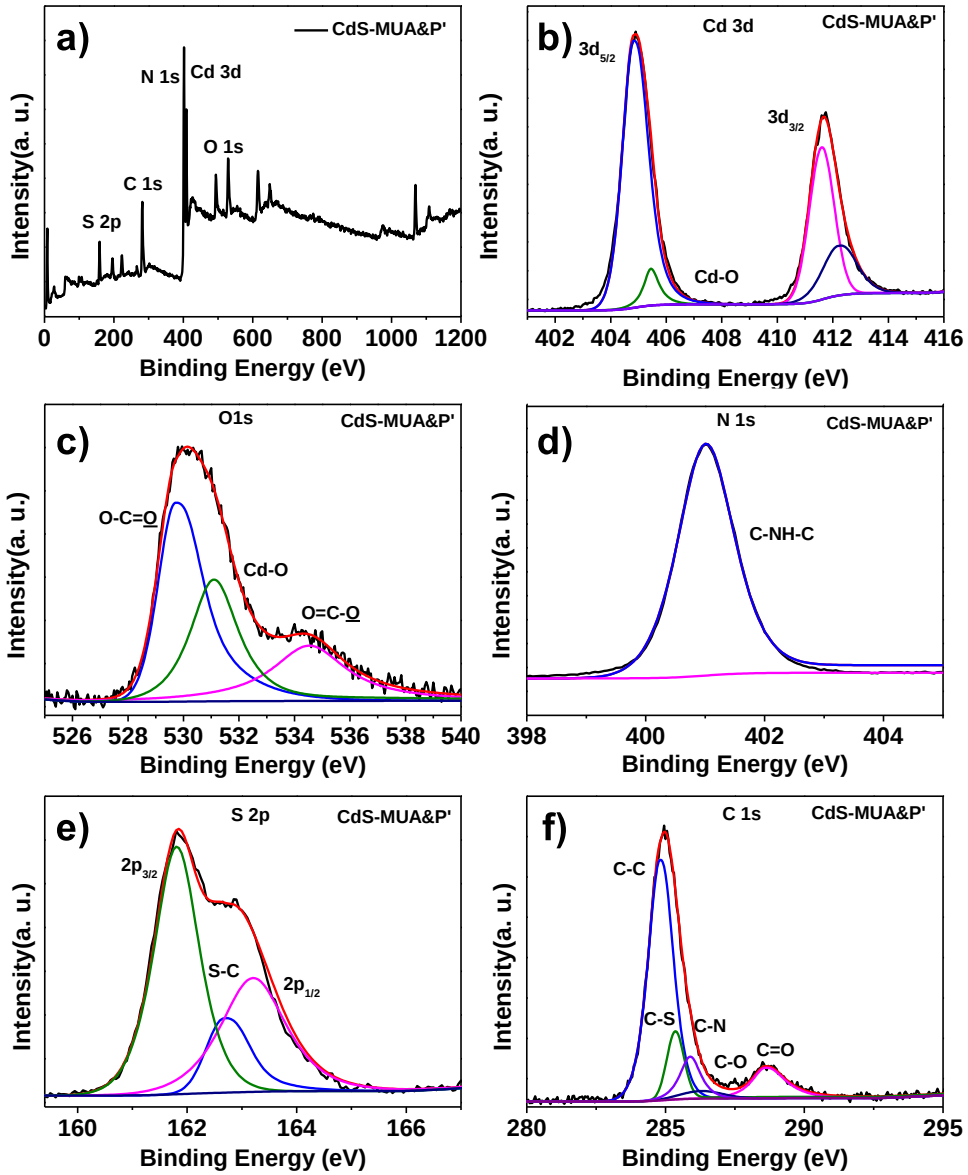

Fig. S11 The XPS spectra of (a) full spectrum, (b) Cd 3d, (c) O 1s, (d) N 1s (e) S 2p and (f) C 1s respectively for **CdS-MUA&P'**.

Fig. S9a showed the full scan of XPS spectra for **CdS-MUA&P'**. The Cd 3d spectrum displayed two peaks at 411.6 and 404.8 eV, which were in line with the binding energy for Cd $3d_{3/2}$ and Cd $3d_{5/2}$ respectively (Fig. S9b).[8] It indicated 6.8 eV binding energy difference, which identified Cd^{2+} was involved in **CdS-MUA&P'**. Further deconvolution led to respective signals at 412.2 and 405.5 eV were assigned to Cd-O bond, which was correlated with the peak at 531.1 eV in O 1s

spectrum (Fig. S9c), implying N-methyl-proline was anchored on QDs surface by Cd-O bond. This was consistent with that for the formation of **CdS-MUA&P** and **CdS-P.** Moreover, the peaks at 529.7 and 534.5 eV in O 1s spectrum can be ascribed to the binding energy of O-C=O, O=C-O. The N 1s spectrum displayed peak at 401.0 eV (Fig. S9d). The S 2p spectrum exhibited peaks at 163.2 and 161.8 eV (Fig. S9e), which were the typical signals belonged to metallic sulfides, accompanied by a peak at 162.7 eV ascribed to S-C bond on MUA chain.[8] The C 1s spectrum displayed five peaks at 284.8, 285.4, 285.9, 286.3 and 288.6 eV (Fig. S9f), which corresponded to C-C, C-S, C-N, C-O and C=O respectively. Therefore, **CdS-MUA&P'** exhibited the analogous bond connection to **CdS-MUA&P** based on XPS.

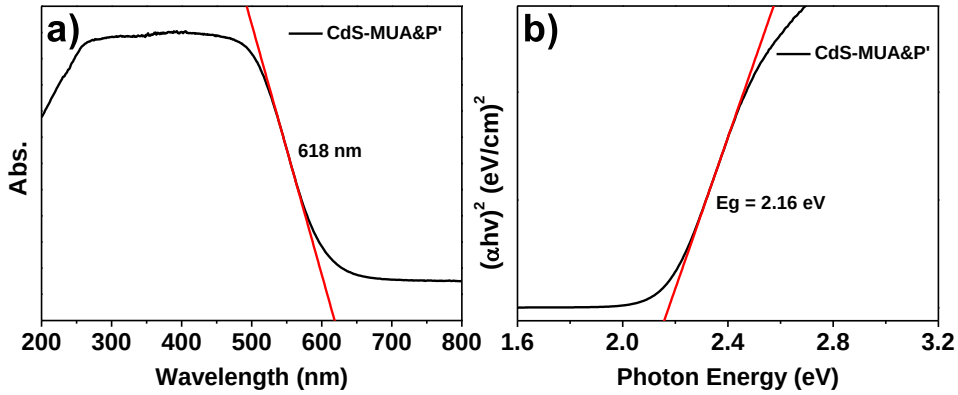

Fig. S12 a) The UV-vis DRS spectra of **CdS-MUA&P'**; b) the corresponding Tauc plots $(ahv)^2$ plots versus hv.

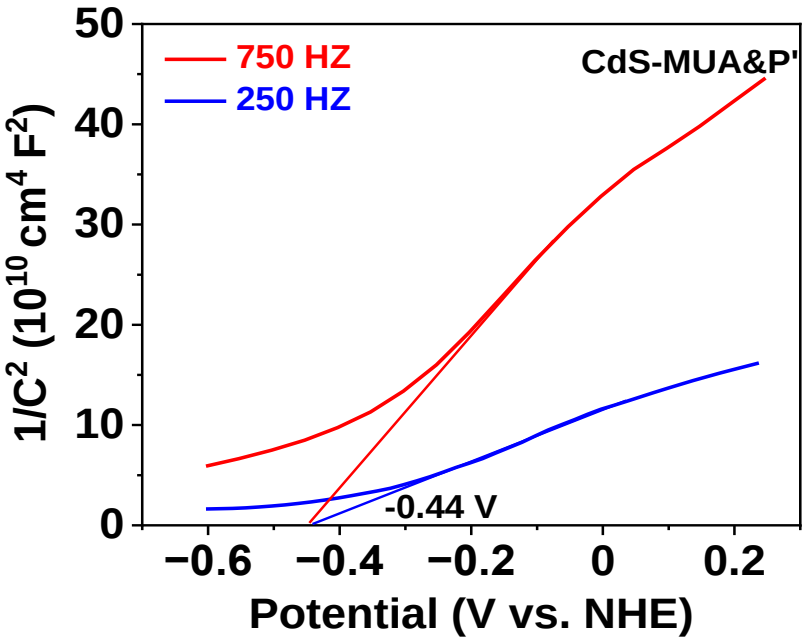

Fig. S13. The Mott-Schottky (MS) curves for determining the band location of **CdS-MUA&P'**.

As shown in Fig. S13, **CdS-MUA&P'** displayed the position of CB at -0.44 eV. Based on the E_g estimated from UV-vis DRS spectra in Fig. S12, the VB were located at 1.72 eV.

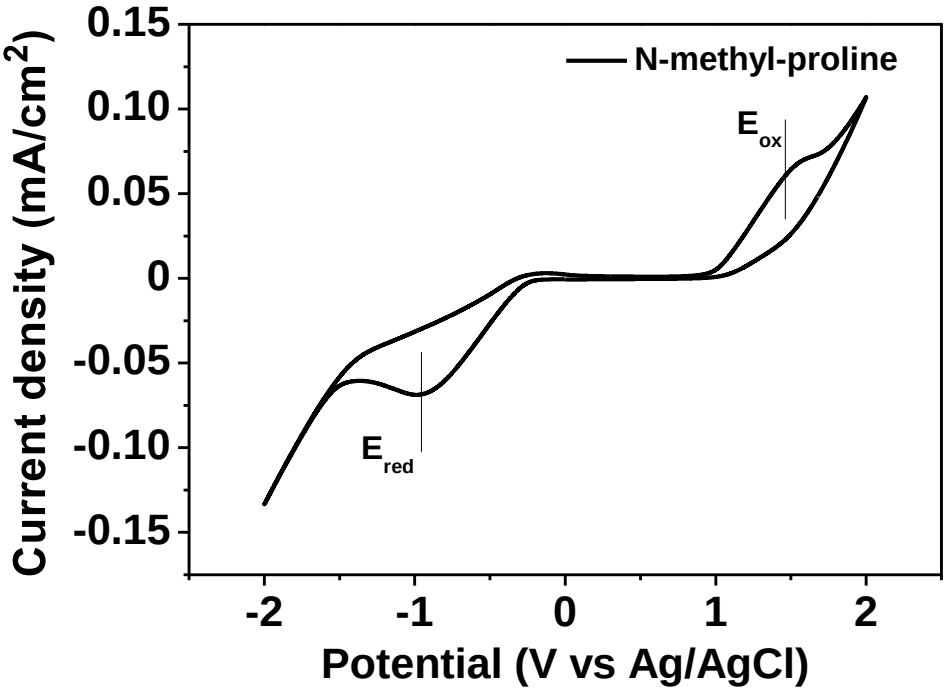

Fig. S14 CV spectrum of N-methyl-proline, which was carried out with bare FTO electrode as working electrode, Ag/AgCl electrode as reference and graphite rod as a counter electrode.[7]

Based on equation (6), the HOMO level of N-methyl-proline was calculated at 1.67 V.

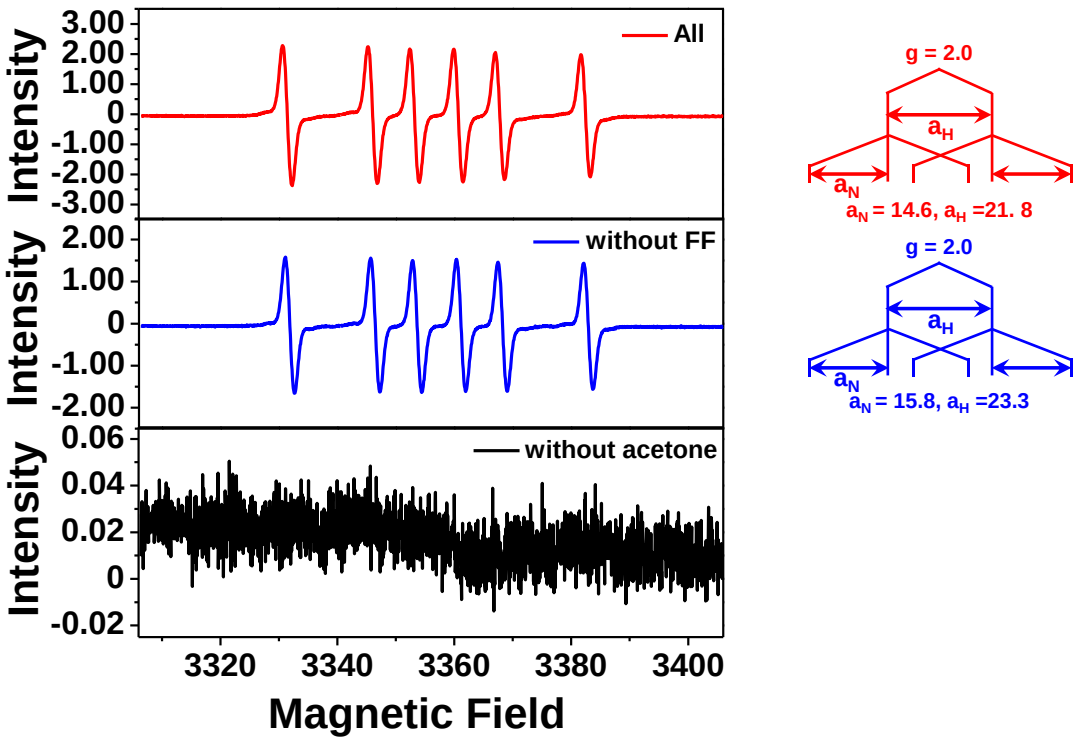

Fig. S15 Experimental EPR spectra of the reaction mixture under irradiation. Condition: 2 mL acetone/H_2O mixture, **CdS-MUA&P** (2 mg mL^{-1}), TEA (1.6 M), DMPO (0.12 M) with or without FF (0.2 M) under LED irradiation (λ = 420 nm) for 10 min under N_2 at room temperature. In the system without acetone, H_2O was added to guarantee each component under the same concentration.

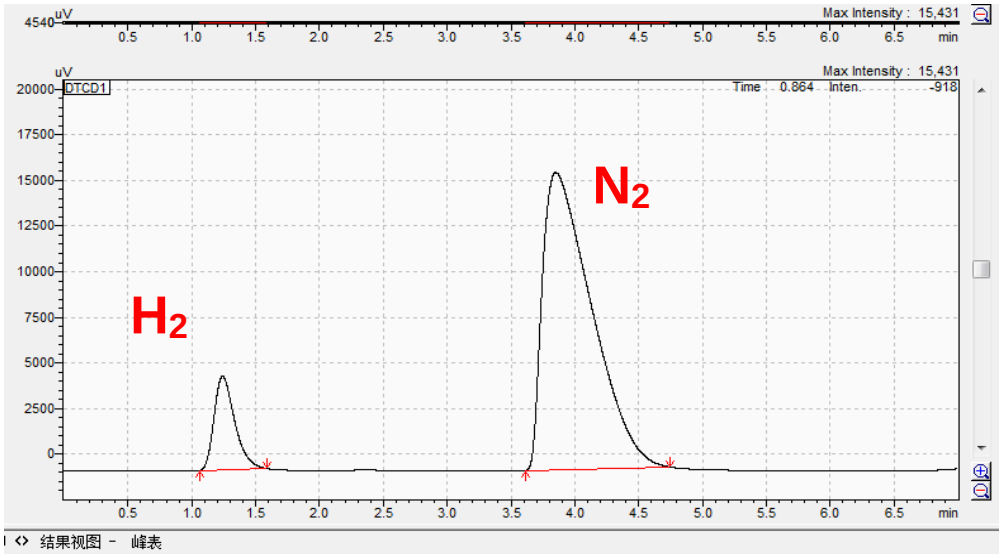

Fig. S16 The GC spectrum of gas composition measured by photocatalytic system using **CdS-MUA&P** as catalyst, in which Ar was applied as carrier gas, and the hydrogen production was calculated as 124 μmol g_{cat}^{-1} h^{-1} through external standard method.

Table S1 The effect of acetone and water ratio for aldol condensation of FF with acetone by **CdS-MUA&P**.

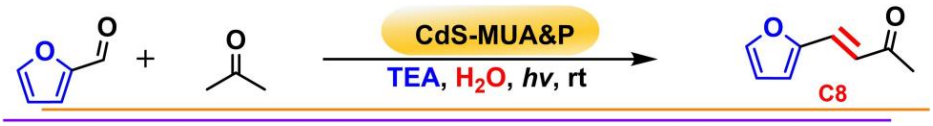

Entry	Acetone : H_2O	Yield (%)	Conversion (%)
1	1 : 1	60.9	81.4
2	1.5 : 0.5	98.9	100
3	0.5 : 1.5	47.8	54.2

Table S2. The control for the reaction of FF and acetone under the standard conditions.

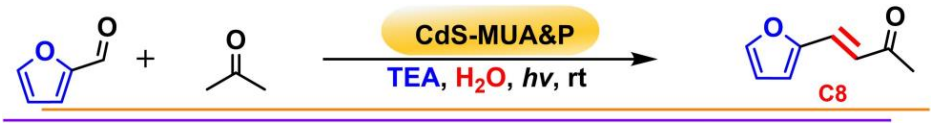

Entry	photocatalyst	TEA	light	Yield (%)	Conversation (%)
1	CdS-MUA&P	√	×	27.2%	29.6%
2	CdS-MUA&P	×	√	0	0
3	×	√	√	23.1%	25.8%

Table S3. Recycling experiments for aldol condensation of FF and acetone with **CdS-MUA&P** as the photocatalyst under the standard condition.

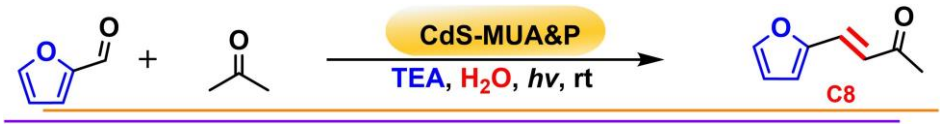

Entry	Recycle Times	Yield (%)	Conversion (%)
1	0	98.9	100
2	1	80.7	94.3
3	2	62.2	87.1
4	3	51.1	72.8

Table S4. The time-resolved photoluminescence lifetime of **CdS-MUA&P**, **CdS-MUA** and **CdS-P** respectively.

Entry	Photocatalyst	Short lifetime (τ_1)	Long lifetime (τ_2)	Average lifetime (τ)
1	**CdS-MUA&P**	1.1 ns	9.1 ns	7.6 ns
2	**CdS-MUA**	1.5 ns	14.8 ns	12.9 ns
3	**CdS-P**	1.2 ns	13.5 ns	11.8 ns

Table S5. The conduction band and valence band of **CdS-MUA&P**, **CdS-MUA&P'**, **CdS-MUA** and **CdS-P** respectively.

Entry	Photocatalyst	Band Gap (eV)	Conduction Band (V)	Valence Band (V)
1	**CdS-MUA&P**	2.13	-0.39	1.74
2	**CdS-MUA&P'**	2.16	-0.40	1.76
3	**CdS-MUA**	2.08	-0.36	1.72
4	**CdS-P**	2.19	-0.42	1.77

The determination for the CB and VB of CDs were based on the band gap of catalysts, which were according to the following equations:[9]

$$E_{CB} = \chi - E^e - 1/2E_g \quad (7)$$

$$E_{VB} = E_g + E_{CB} \quad (8)$$

Here, E_{CB} is the CB edge potential, E_{VB} is the VB edge potential, E_g is the band gap of CDs, which determined from UV-vis DRS (Fig. S4 and Fig. S10). χ represents the electronegativity of the semiconductor, expressed as the geometric mean of the absolute electronegativity of the constituent atoms, which is defined as the arithmetic mean of the atomic electron affinity and the first ionization energy.[9] E^e is the energy of free electrons on the hydrogen scale ≈4.5 eV.

Visibly, the evaluation of energy-band position based on calculation is very close to those determined from M-S curves in Fig. S7 and Fig. S13. Therefore, the two methods can be mutually authenticated.

Table S6. Radical mechanism tests for aldol condensation of FF and acetone with **CdS-MUA&P** as the photocatalyst in the presence of TBC under the standard conditions.

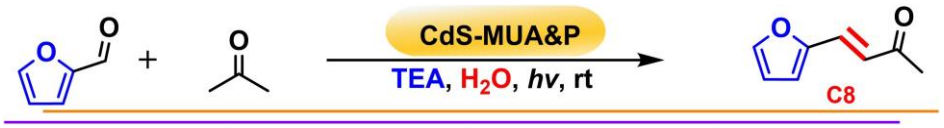

Entry	TBC addition (mmol)	Yield (%)	Conversion (%)
1	0	98.9	100
2	0.25	41.7	53.1
3	0.50	29.3	41.9
4	1.00	2.8	9.1

3. Supporting Spectroscopic Data

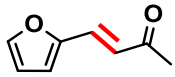

4-(furan-2-yl)but-3-en-2-one (C8): The crude product was purified by TLC isolation with eluent (petroleum ether: acetone= 15: 1) to afford **C8** in 98.9% yield (134 mg); ^{1}H NMR (600 MHz, Chloroform-*d*): δ = 7.50 (d, *J* = 1.8 Hz, 1H), 7.28 (d, *J* = 16.0 Hz, 1H), 6.67 (d, *J* = 3.5 Hz, 1H), 6.61 (dd, *J* = 15.9, 1.6 Hz, 1H), 6.49 (dt, *J* = 3.3, 1.6 Hz, 1H), 2.32 (d, *J* = 1.5 Hz, 3H); ^{13}C NMR (600 MHz, Chloroform-*d*): δ = 197.74, 150.87, 145.01, 129.39, 124.28, 115.62, 112.53, 30.85, 27.78; HRMS (ESI): m/z calculated for $C_8H_8O_2$ $[M + Na]^+$: 159.0417; found: 159.0417.

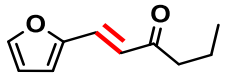

1-(furan-2-yl)hex-1-en-3-one (C10): The crude product was purified by TLC isolation with eluent (petroleum ether : acetone = 30: 1) to afford **C10** in 65.4% yield (107 mg); ^{1}H NMR (400 MHz, Chloroform-*d*): δ = 7.46 (d, *J* = 1.8 Hz, 1H), 7.29 (d, *J* = 15.9 Hz, 1H), 6.68-6.55 (m, 2H), 6.45 (dd, *J* = 3.4, 1.8 Hz, 1H), 2.55 (t, *J* = 7.4 Hz, 2H), 1.66 (h, *J* = 7.4 Hz, 2H), 0.93 (t, *J* = 7.4 Hz, 3H); ^{13}C NMR (400 MHz, Chloroform-*d*): δ = 200.23, 151.21, 144.89, 128.56, 123.50, 115.62, 112.59, 43.39, 17.91 13.91; HRMS (ESI): m/z calculated for $C_{10}H_{12}O_2$ $[M + Na]^+$: 187.0730; found: 187.0723.

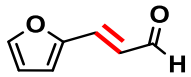

3-(furan-2-yl)acrylaldehyde (C7): The crude product was purified by TLC isolation with eluent (petroleum ether : ethyl acetate = 3 : 1) to afford **C7** in 74.3% yield (91 mg); ^{1}H NMR (400 MHz, Chloroform-*d*): δ = 9.62 (d, *J* = 7.9 Hz, 1H),

7.57 (s, 1H), 7.23 (d, *J* = 15.7 Hz, 1H), 6.78 (d, *J* = 3.5 Hz, 1H), 6.66-6.49 (m, 2H); ^{13}C NMR (400 MHz, Chloroform-*d*): δ = 192.90, 150.60, 145.93, 137.83, 126.00, 116.75, 112.89; HRMS (ESI): m/z calculated for $C_7H_6O_2$ $[M + Na]^+$: 145.0260; found: 145.0256.

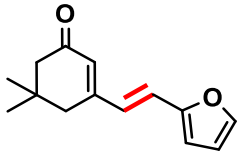

6-(furan-2-ylmethylene)-3,5,5-trimethylcyclohex-2-en-1-one (C14): The crude product was purified by TLC isolation with eluent (n-hexane : acetone = 10 : 1) to afford **C14** in 82.0% yield (177 mg); ^{1}H NMR (400 MHz, Chloroform-*d*): δ = 7.41 (d, *J* = 1.8 Hz, 1H), 6.90-6.67 (m, 2H), 6.53-6.31 (m, 2H), 6.01 (s, 1H), 2.36 (s, 2H), 2.25 (s, 2H), 1.05 (s, 6H); ^{13}C NMR (400 MHz, Chloroform-*d*): δ = 200.16, 154.49, 152.39, 143.81, 127.76, 126.95, 122.18, 112.27, 112.03, 51.45, 38.83, 33.37, 28.55; HR-MS (ESI): m/z calculated for $C_{14}H_{16}O_2$ $[M + Na]^+$: 239.1043; found: 239.1033.

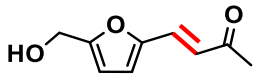

4-(5-(hydroxymethyl)furan-2-yl)but-3-en-2-one (C9): The crude product was purified by TLC isolation with eluent (n-hexane: ethyl acetate = 1 : 1) to afford **C9** in 99.1% yield (164 mg); ^{1}H NMR (400 MHz, Chloroform-*d*): δ = 7.41 (d, *J* = 15.6 Hz, 1H), 6.88 (d, *J* = 15.6 Hz, 1H), 6.62 (d, *J* = 3.4 Hz, 1H), 6.39 (d, *J* = 3.4 Hz, 1H), 4.76-3.82 (m, 3H), 2.09 (d, *J* = 50.9 Hz, 3H); ^{13}C NMR (400 MHz, Chloroform-*d*): δ = 197.92, 156.92, 150.90, 129.32, 124.26, 116.69, 110.54, 57.71, 28.10; HRMS (ESI): m/z calculated for $C_9H_{10}O_3$ $[M + Na]^+$: 189.0522; found:

189.0522.

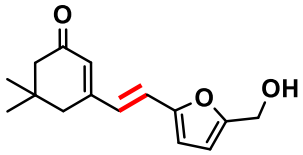

6-((5-(hydroxymethyl)furan-2-yl)methylene)-3,5,5-trimethylcyclohex-2-en-1-one (C15a): The crude product was purified by TLC isolation with eluent (petroleum ether : ethyl acetate = 3 : 1) to afford **C15a** in 71.5% yield (175 mg); ^{1}H NMR (400 MHz, Chloroform-*d*): δ = 6.72 (q, *J* = 16.0 Hz, 2H), 6.37 (d, *J* = 3.3 Hz, 1H), 6.29 (d, *J* = 3.4 Hz, 1H), 5.96 (s, 1H), 4.58 (s, 2H), 3.38 (s, 1H), 2.32 (s, 2H), 2.20 (s, 2H), 1.01 (s, 6H); ^{13}C NMR (400 MHz, Chloroform-*d*): δ = 200.70, 156.11, 155.09, 152.11, 127.50, 126.63, 122.32, 113.23, 110.19, 57.41, 51.28, 38.78, 33.35, 28.49; HRMS (ESI): m/z calculated for $C_{15}H_{18}O_3$ $[M + Na]^+$: 269.1148; found: 269.1143.

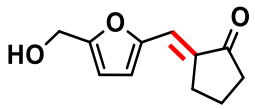

2-((5-(hydroxymethyl)furan-2-yl)methylene)cyclopentan-1-one (C11): The crude product was purified by TLC isolation with eluent (petroleum ether : ethyl acetate = 2 : 1) to afford **C11** in 91.2% yield (175 mg); ^{1}H NMR (400 MHz, Chloroform-*d*): δ = 6.96 (t, *J* = 2.8 Hz, 1H), 6.49 (d, *J* = 3.5 Hz, 1H), 6.29 (d, *J* = 3.5 Hz, 1H), 4.52 (s, 2H), 4.07 (s, 1H), 2.81 (td, *J* = 7.4, 2.7 Hz, 2H), 2.23 (t, *J* = 7.9 Hz, 2H), 1.88 (d, *J* = 7.6 Hz, 2H); ^{13}C NMR (400 MHz, Chloroform-*d*): δ = 208.65, 157.48, 151.73, 133.32, 119.15, 117.25, 110.32, 57.36, 38.03, 29.09, 19.68; HRMS (ESI): m/z calculated for $C_{11}H_{12}O_3$ $[M + Na]^+$: 215.0679; found: 215.0674.

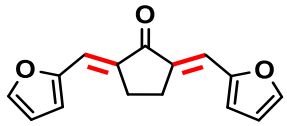

2,5-bis(furan-2-ylmethylene)cyclopentan-1-one (C15b): The crude product was purified by TLC isolation with eluent (petroleum ether : ethyl acetate = 15 : 1) to afford **C15b** in 24.9% yield (60 mg); ^{1}H NMR (600 MHz, Chloroform-*d*): δ = 7.59 (s, 2H), 7.35 (s, 2H), 6.70 (s, 2H), 6.54 (d, *J* = 1.7 Hz, 2H), 3.08 (s, 4H); ^{13}C NMR (400 MHz, Chloroform-*d*): δ = 195.39, 152.79, 145.04, 135.90, 119.85, 115.95, 112.63, 53.42, 25.81; HRMS (ESI): m/z calculated for $C_{15}H_{12}O_3$ $[M + Na]^+$: 263.0682; found: 263.0679.

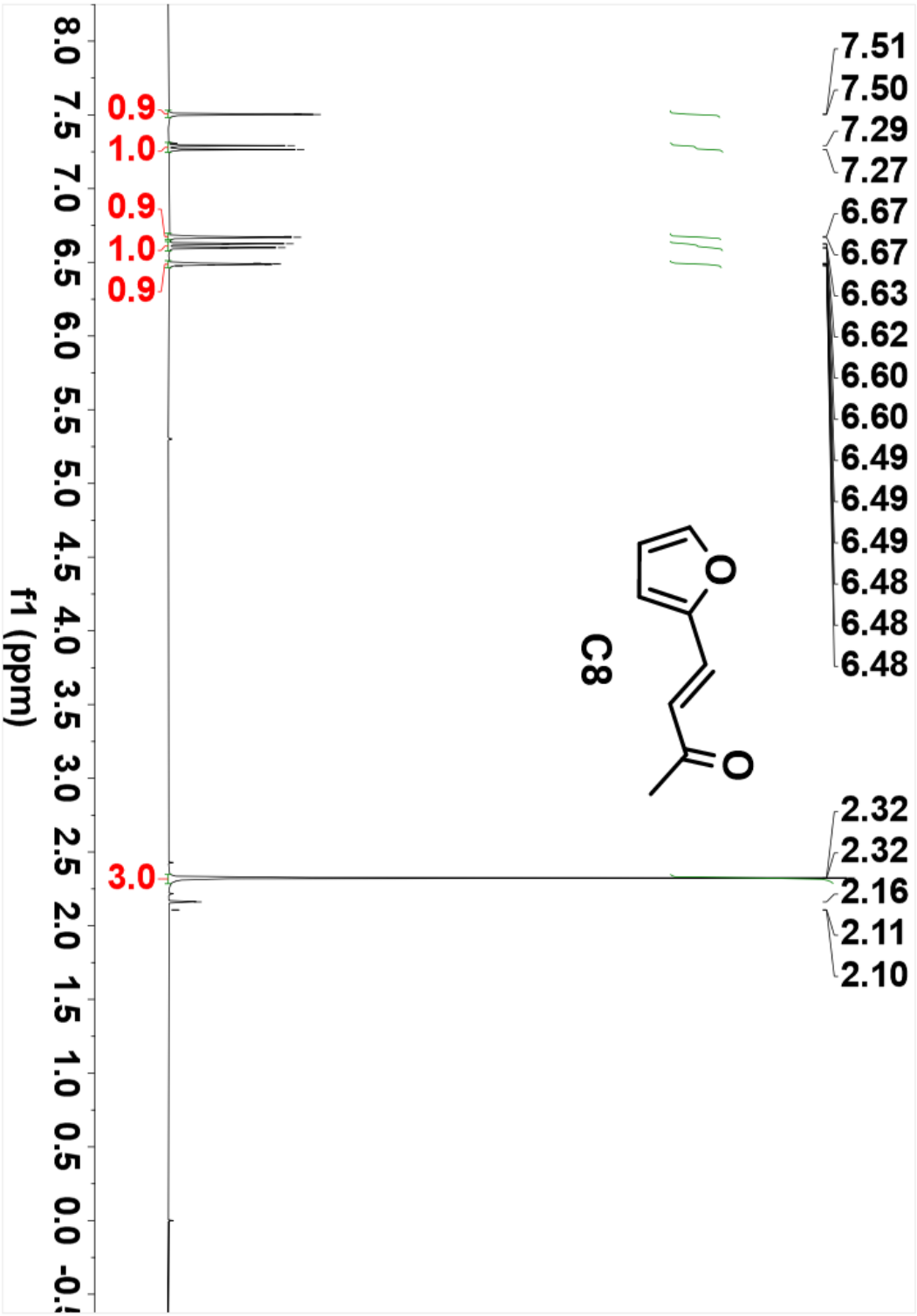
7.51
7.50
7.29
7.27
6.67
6.67
6.63
6.62
6.60
6.60
6.49
6.49
6.49
6.48
6.48
6.48
2.32
2.32
2.16
2.11
2.10
0.9
1.0
0.9
1.0
0.9
3.0
C8
O
O
f1 (ppm)
8.0 7.5 7.0 6.5 6.0 5.5 5.0 4.5 4.0 3.5 3.0 2.5 2.0 1.5 1.0 0.5 0.0

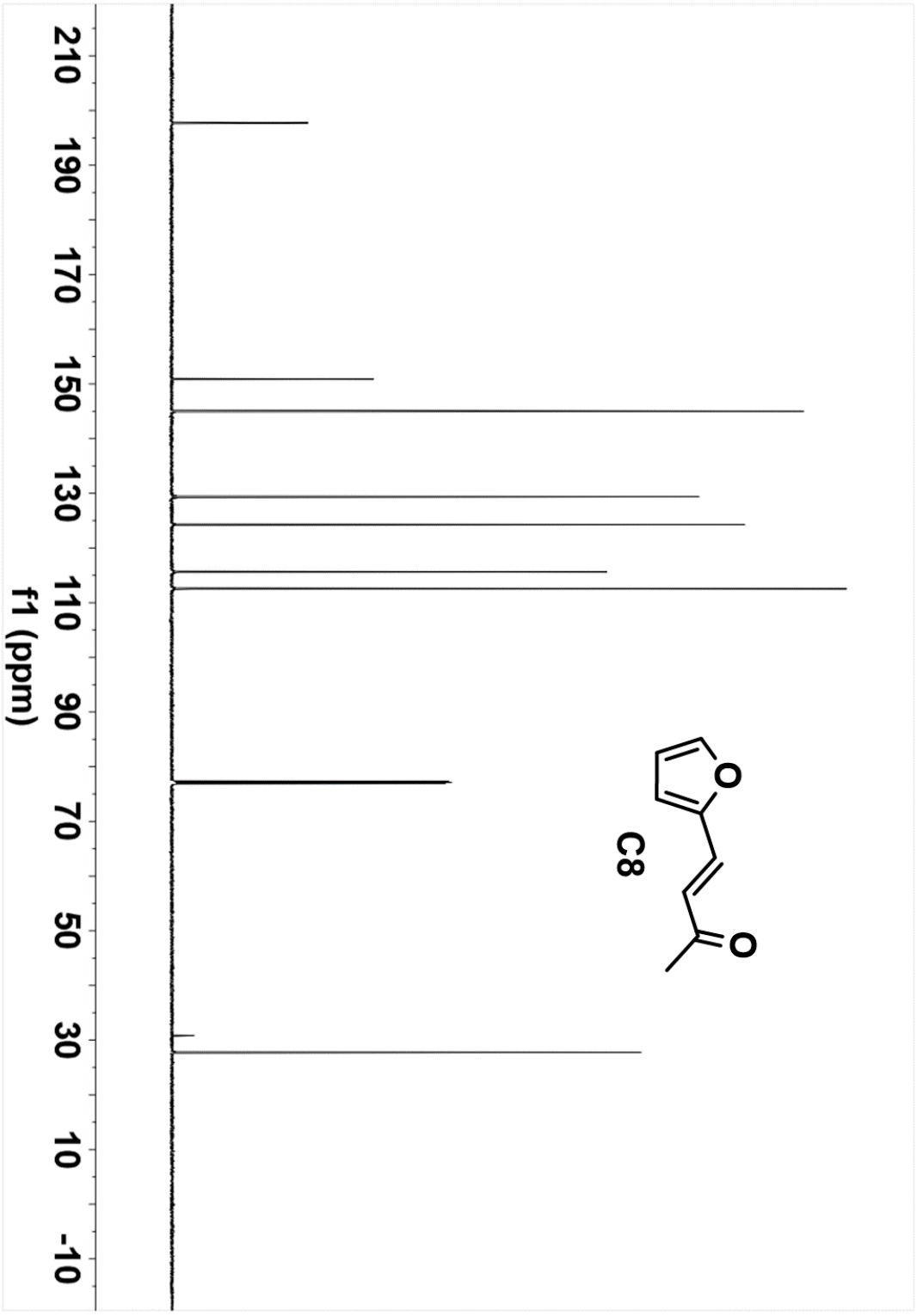
210
190
170
150
130
110
90
70
50
30
10
-10
f1 (ppm)
O
C8
O

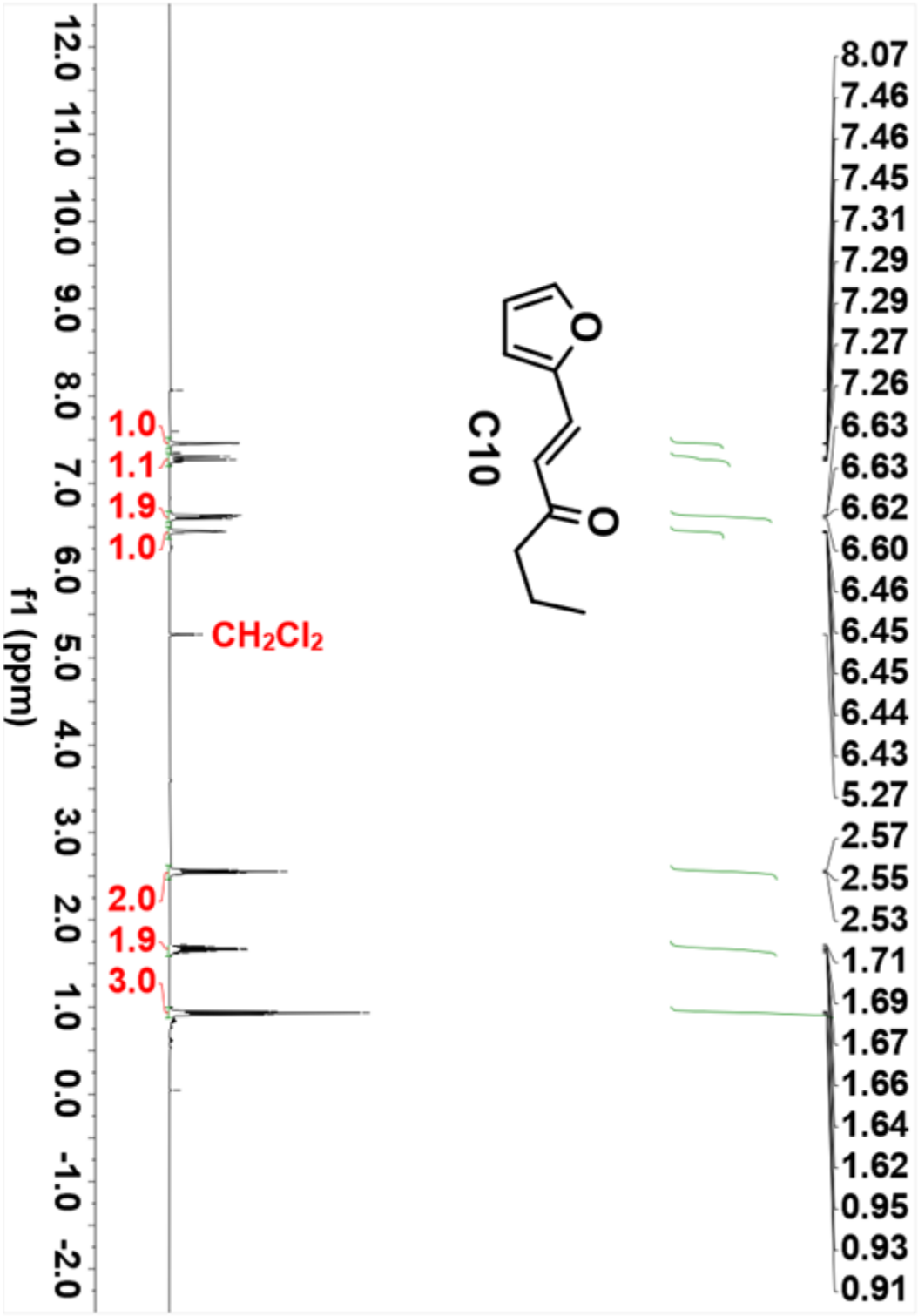
12.0 11.0 10.0 9.0 8.0 7.0 6.0 5.0 4.0 3.0 2.0 1.0 0.0 -1.0 -2.0
f1 (ppm)
1.0
1.1
1.9
1.0
CH2Cl2
2.0
1.9
3.0
C10
O
O
8.07
7.46
7.46
7.45
7.31
7.29
7.29
7.27
7.26
6.63
6.63
6.62
6.60
6.46
6.45
6.45
6.44
6.43
5.27
2.57
2.55
2.53
1.71
1.69
1.67
1.66
1.64
1.62
0.95
0.93
0.91

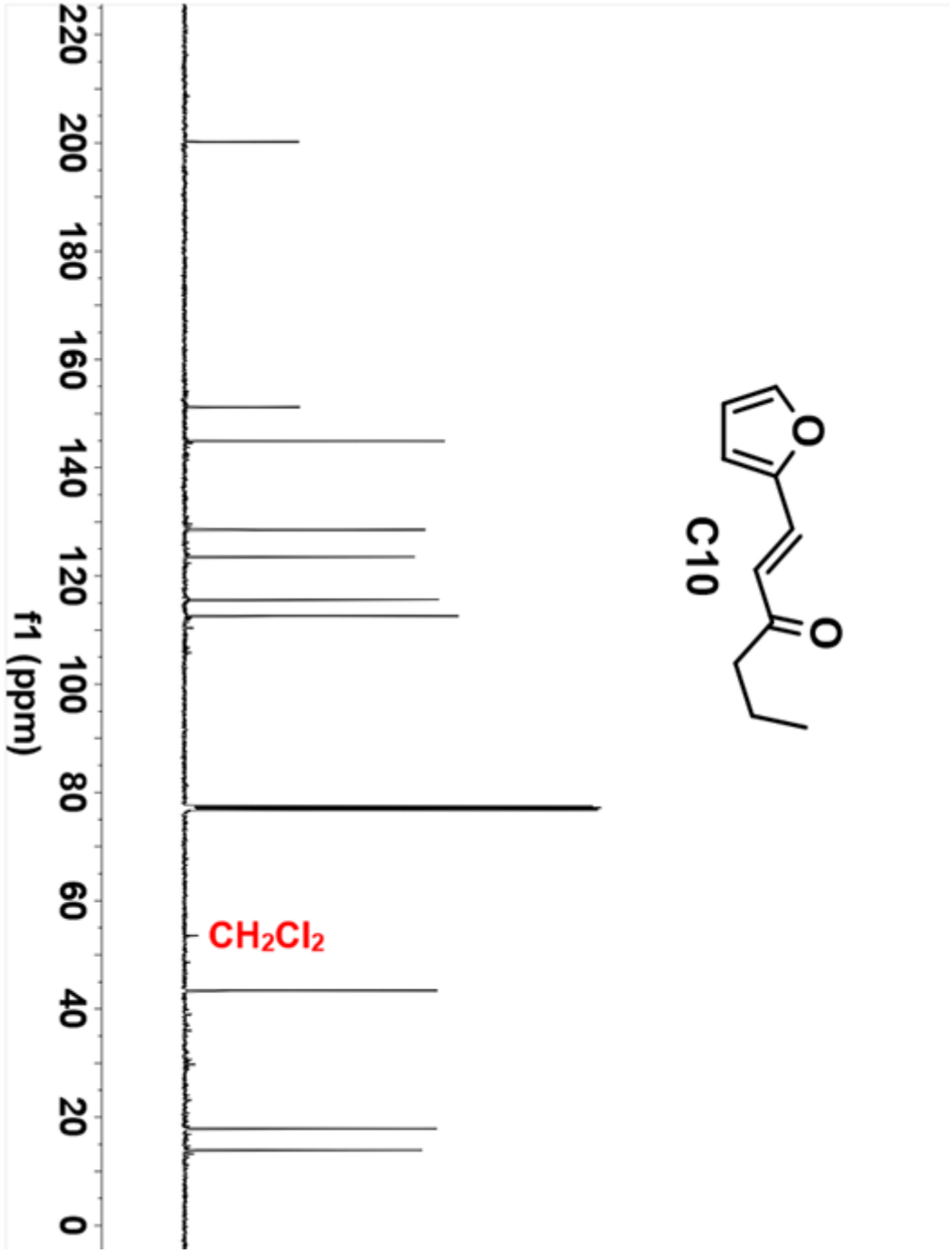
C10
O
O
CH2Cl2
f1 (ppm)
220
200
180
160
140
120
100
80
60
40
20
0

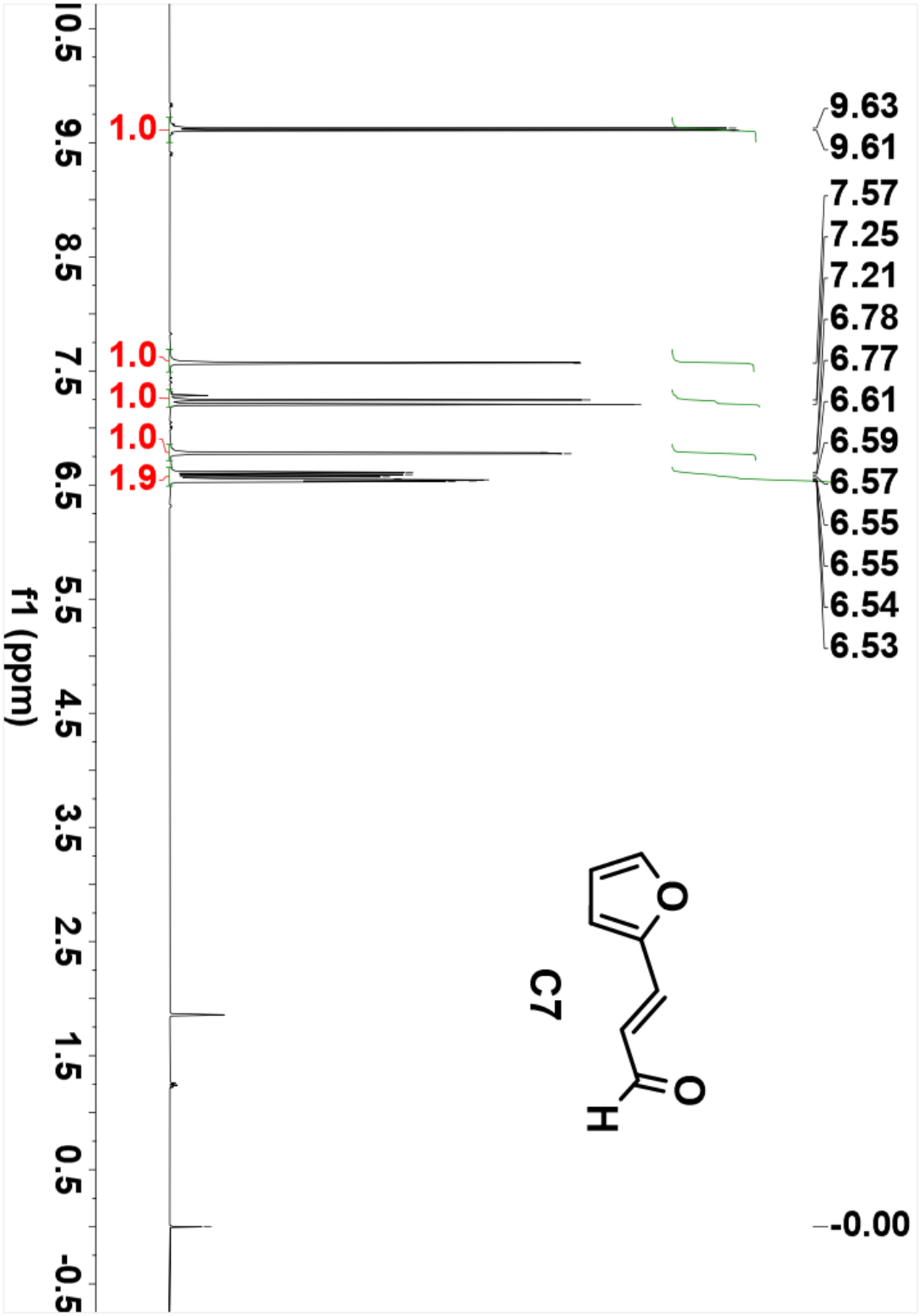
10.5
9.5
8.5
7.5
6.5
5.5
4.5
3.5
2.5
1.5
0.5
-0.5
f1 (ppm)
1.0
1.0
1.0
1.9
9.63
9.61
7.57
7.25
7.21
6.78
6.77
6.61
6.59
6.57
6.55
6.55
6.54
6.53
-0.00
C7
O
O
H

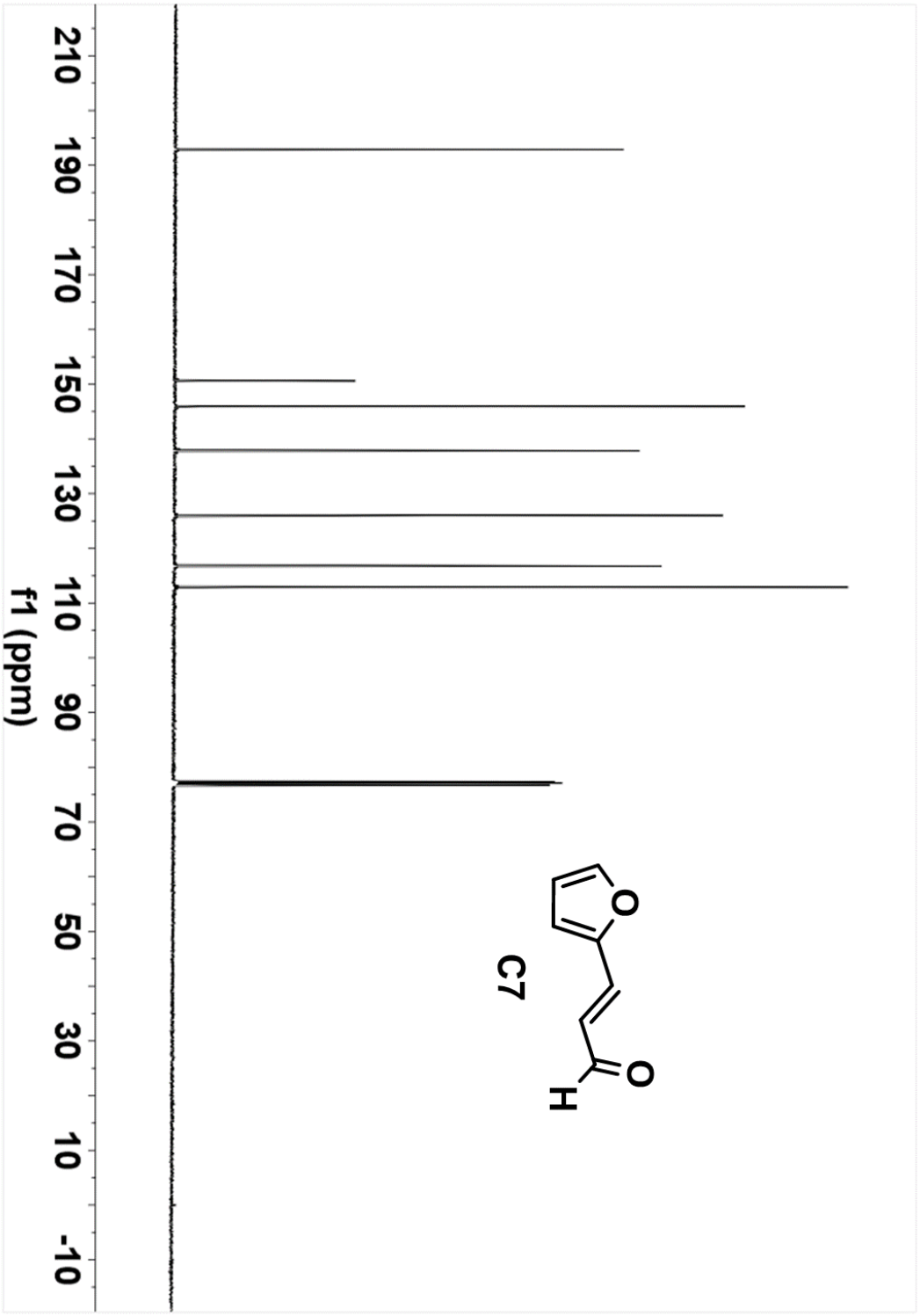
210
190
170
150
130
110
90
70
50
30
10
-10
f1 (ppm)
O
C7
O
H

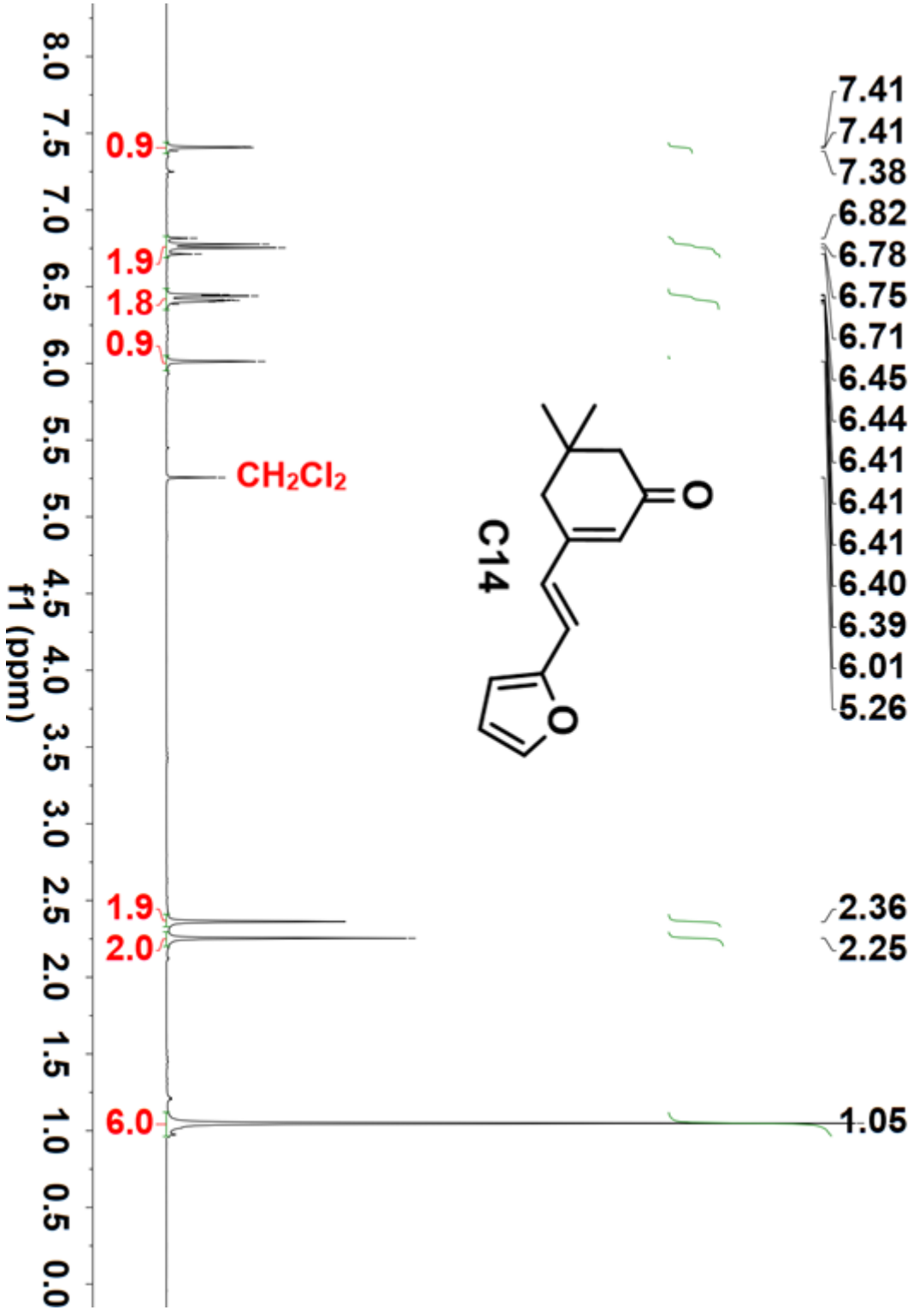
8.0 7.5 7.0 6.5 6.0 5.5 5.0 4.5 4.0 3.5 3.0 2.5 2.0 1.5 1.0 0.5 0.0
f1 (ppm)
0.9
1.9
1.8
0.9
CH2Cl2
1.9
2.0
6.0
C14
O
O
7.41
7.41
7.38
6.82
6.78
6.75
6.71
6.45
6.44
6.41
6.41
6.41
6.40
6.39
6.01
5.26
2.36
2.25
1.05

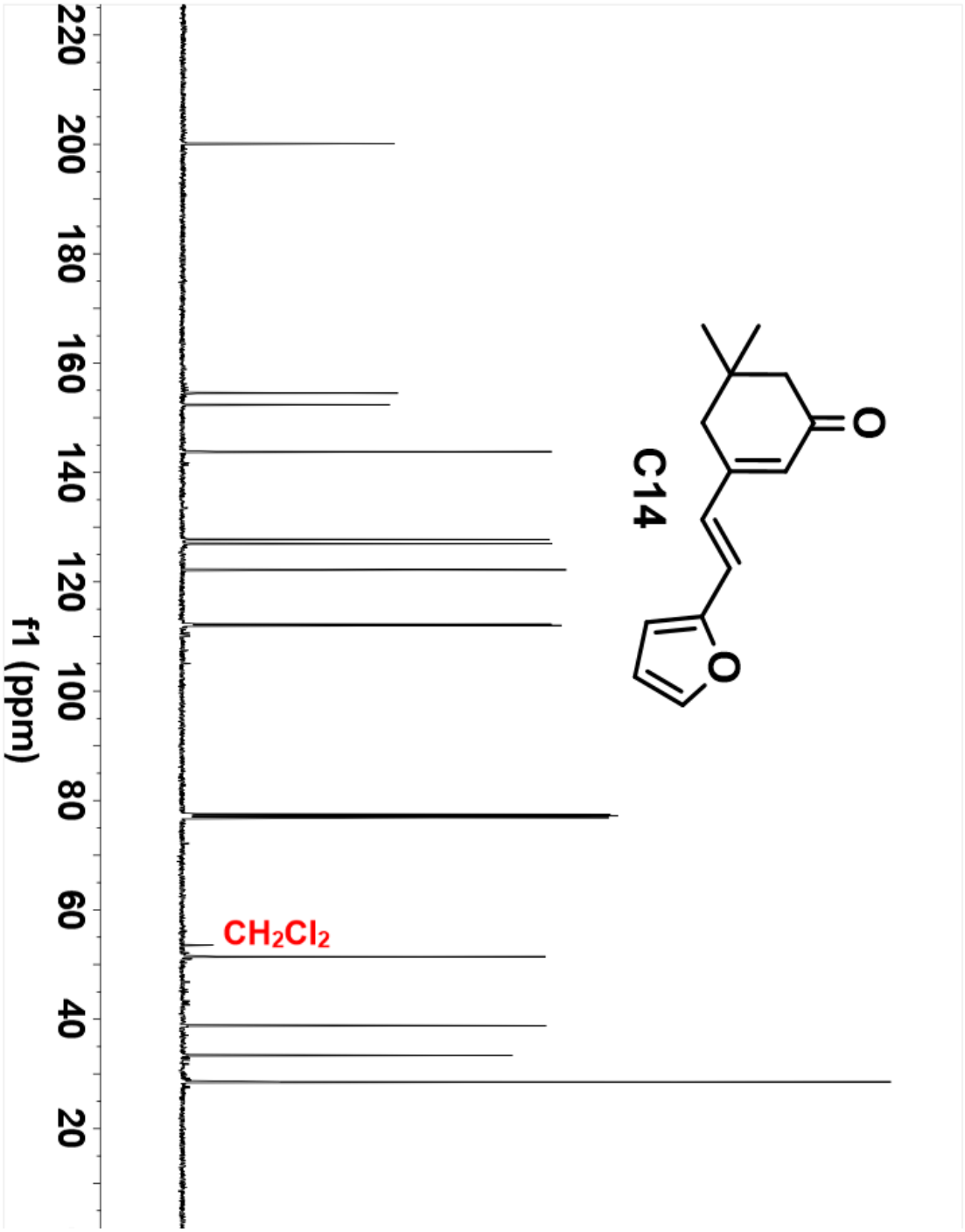
220
200
180
160
140
120
100
80
60
40
20
f1 (ppm)
CH2Cl2
C14
O
O

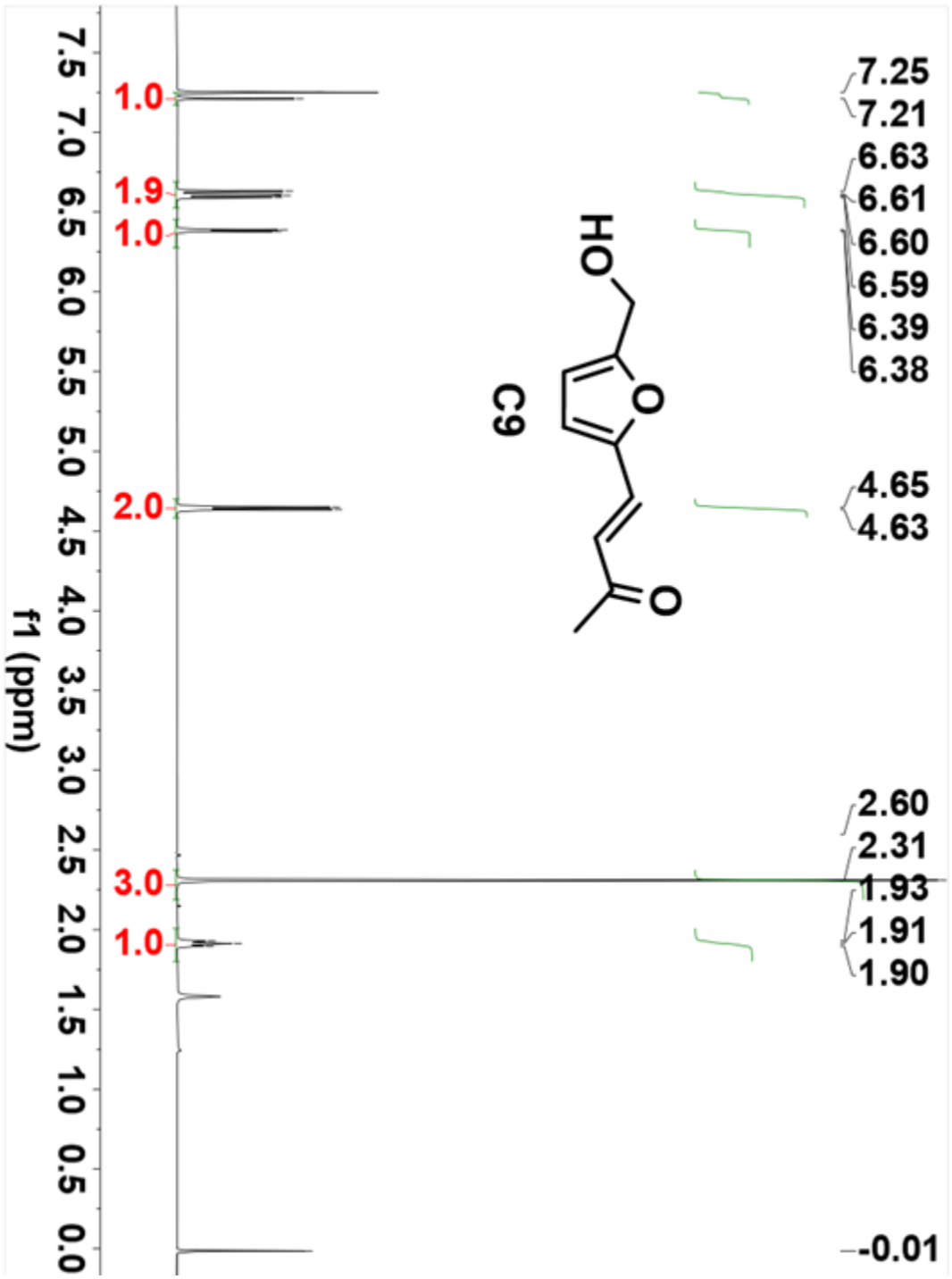
7.25
7.21
6.63
6.61
6.60
6.59
6.39
6.38
4.65
4.63
2.60
2.31
1.93
1.91
1.90
-0.01
1.0
1.9
1.0
2.0
3.0
1.0
HO
O
O
C9
f1 (ppm)

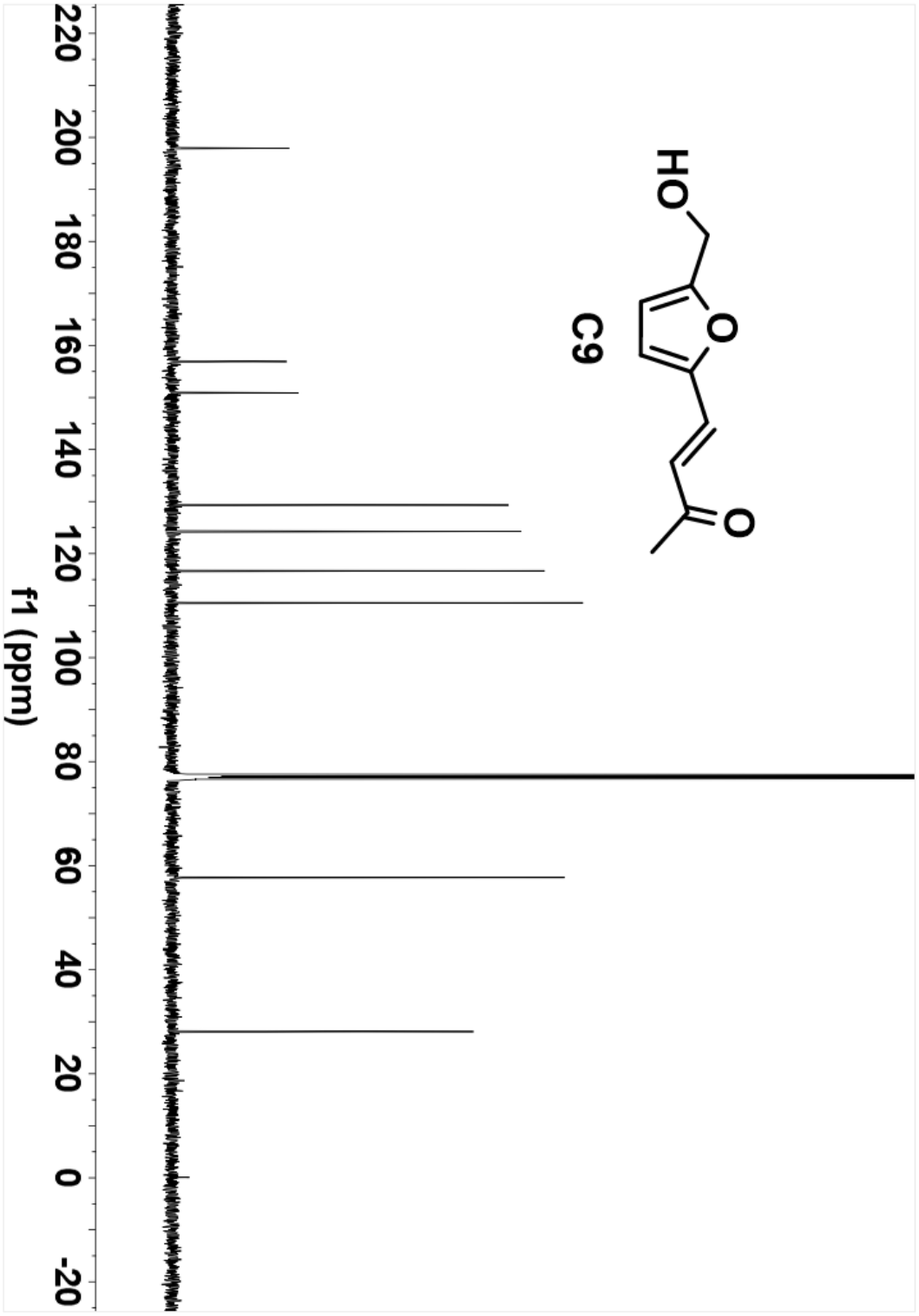
HO
O
O
C9
220
200
180
160
140
120
100
80
60
40
20
0
-20
f1 (ppm)

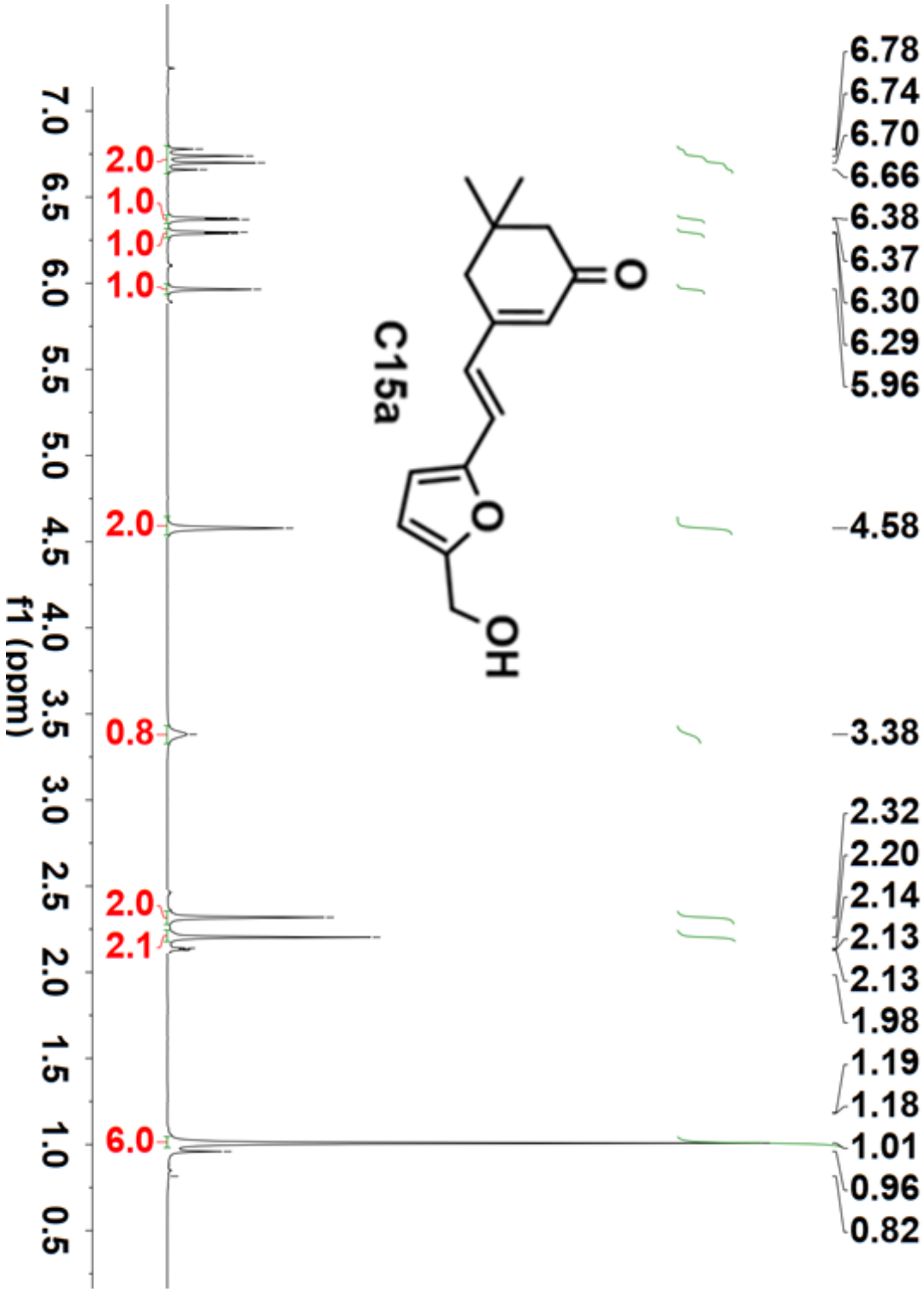
C15a
O
O
OH
f1 (ppm)
7.0
6.5
6.0
5.5
5.0
4.5
4.0
3.5
3.0
2.5
2.0
1.5
1.0
0.5
2.0
1.0
1.0
1.0
2.0
0.8
2.0
2.1
6.0
6.78
6.74
6.70
6.66
6.38
6.37
6.30
6.29
5.96
4.58
3.38
2.32
2.20
2.14
2.13
2.13
1.98
1.19
1.18
1.01
0.96
0.82

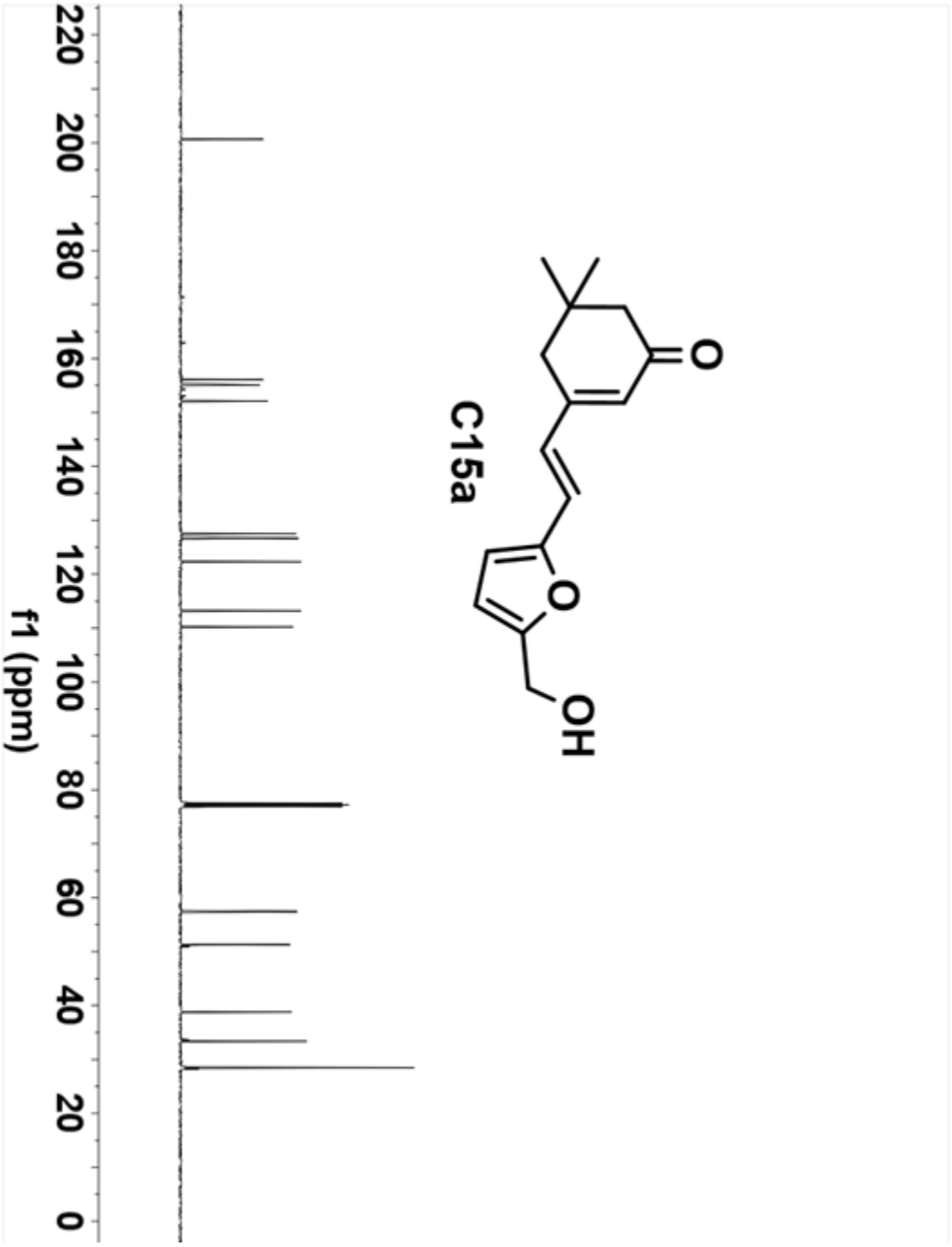
C15a
O
O
OH
f1 (ppm)
220
200
180
160
140
120
100
80
60
40
20
0

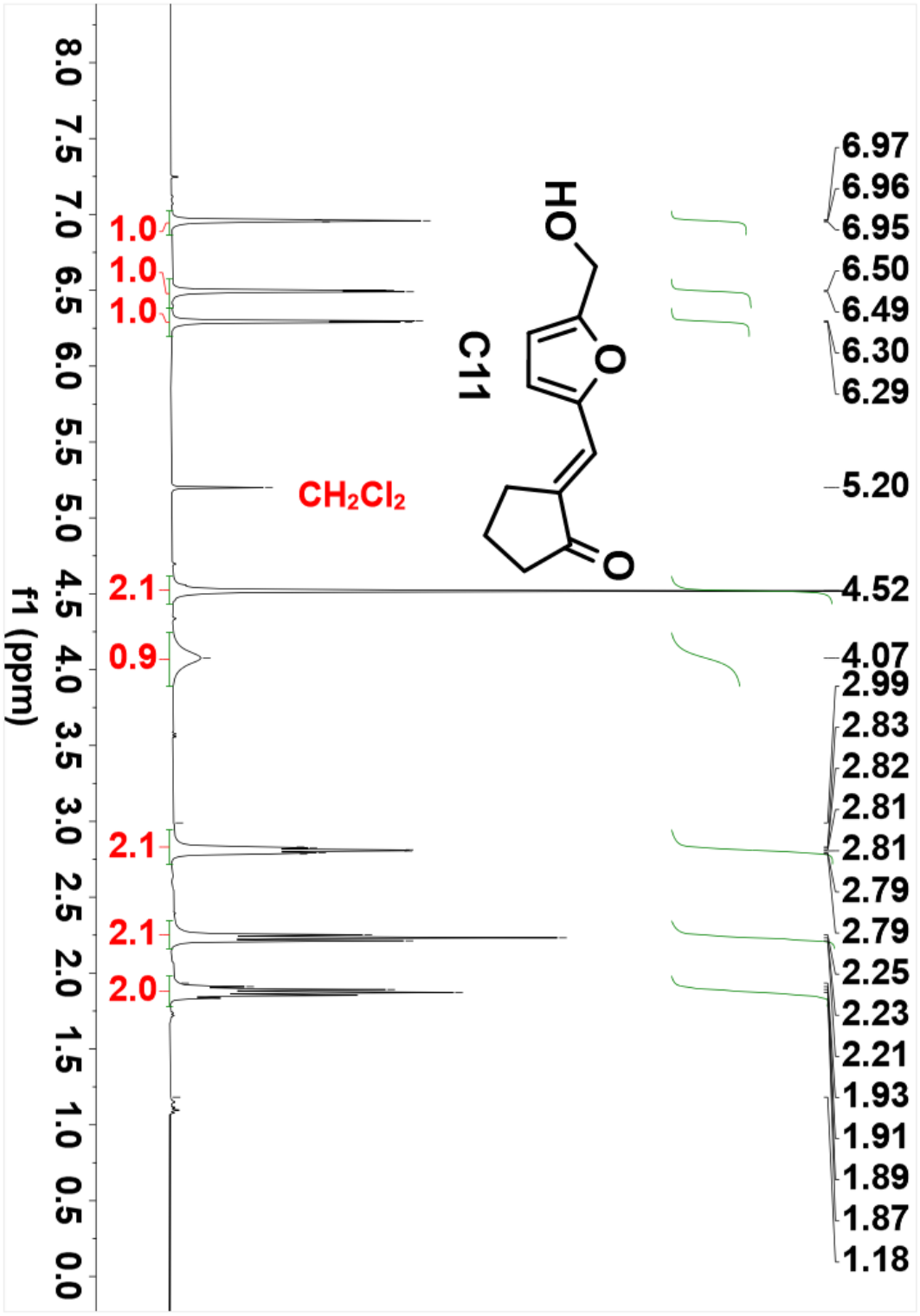
C11
HO
O
O
CH2Cl2
1.0
1.0
1.0
2.1
0.9
2.1
2.1
2.0
6.97
6.96
6.95
6.50
6.49
6.30
6.29
5.20
4.52
4.07
2.99
2.83
2.82
2.81
2.81
2.79
2.79
2.25
2.23
2.21
1.93
1.91
1.89
1.87
1.18
f1 (ppm)
8.0 7.5 7.0 6.5 6.0 5.5 5.0 4.5 4.0 3.5 3.0 2.5 2.0 1.5 1.0 0.5 0.0

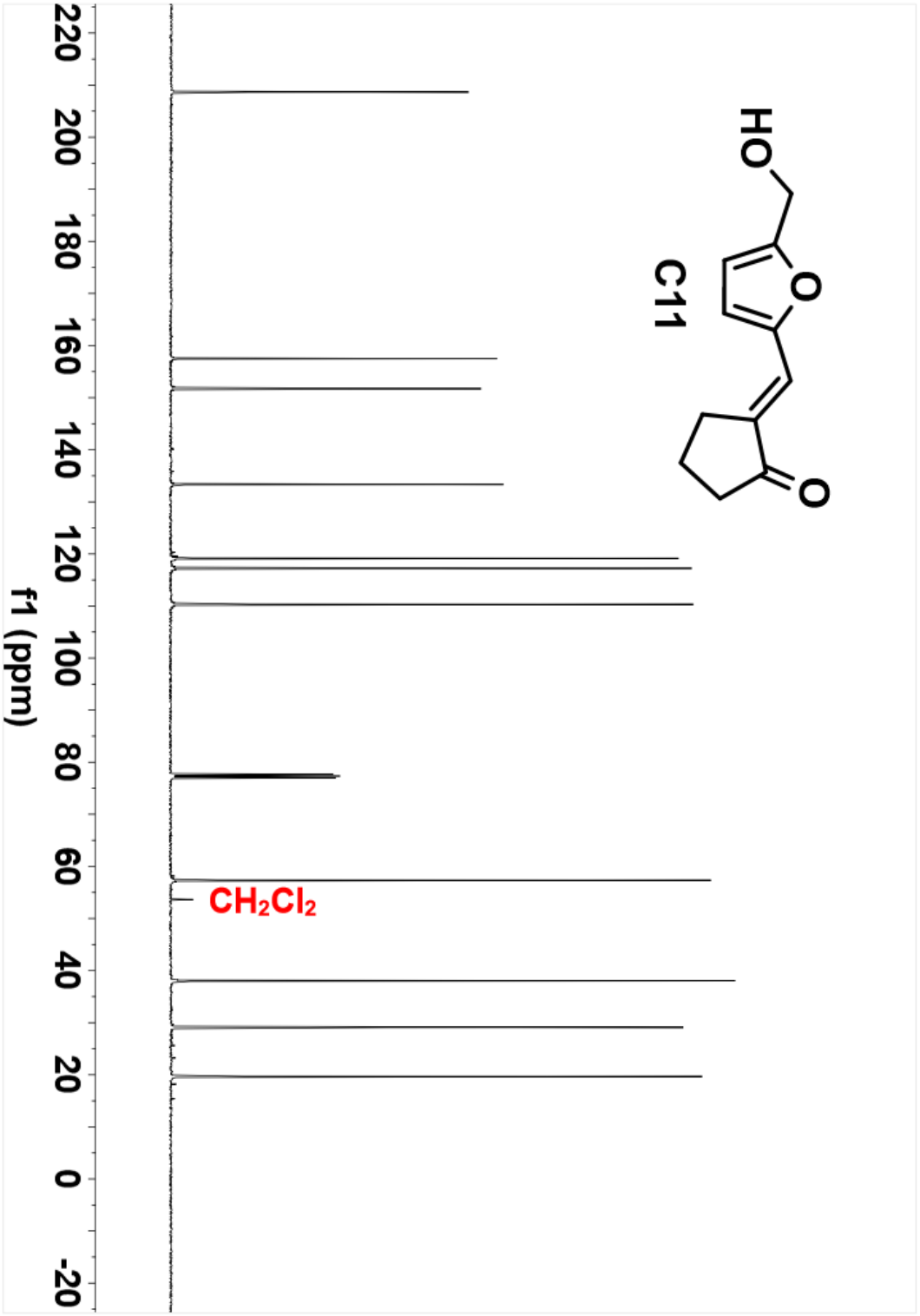
HO
O
O
C11
CH2Cl2
f1 (ppm)
220
200
180
160
140
120
100
80
60
40
20
0
-20

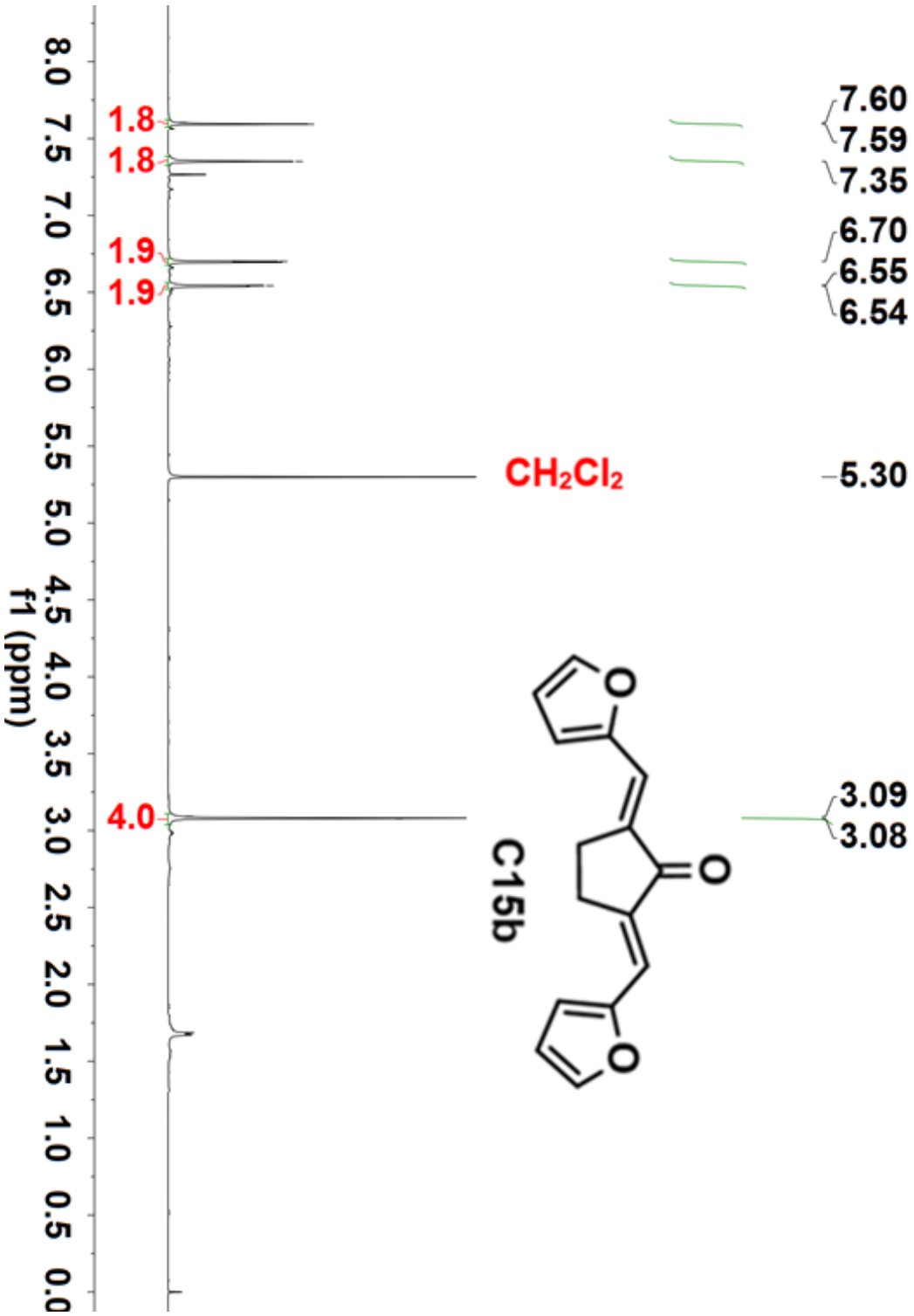
8.0 7.5 7.0 6.5 6.0 5.5 5.0 4.5 4.0 3.5 3.0 2.5 2.0 1.5 1.0 0.5 0.0
f1 (ppm)
1.8
1.8
1.9
1.9
4.0
CH2Cl2
7.60
7.59
7.35
6.70
6.55
6.54
5.30
3.09
3.08
C15b
O
O
O

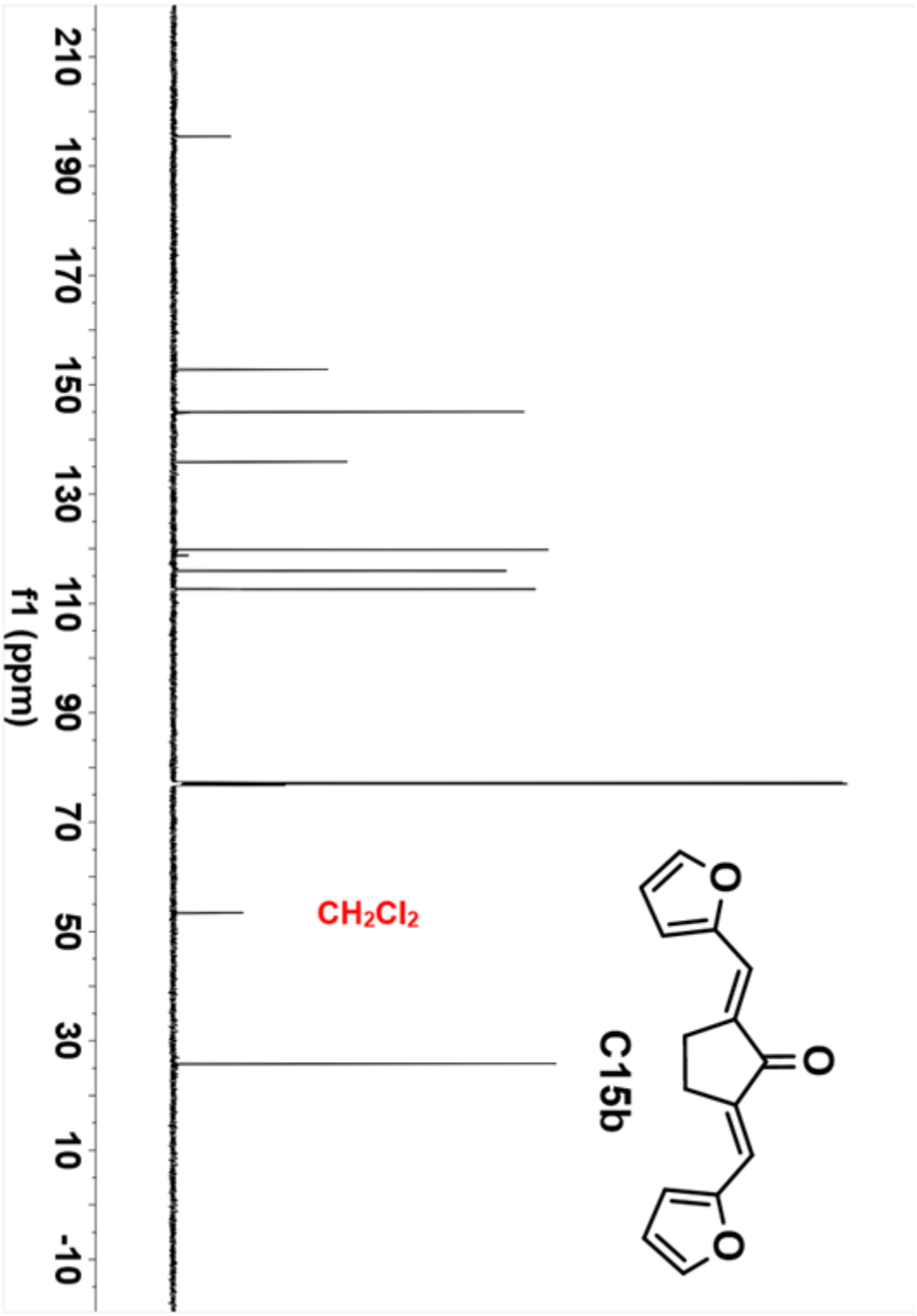
210
190
170
150
130
110
90
70
50
30
10
-10
f1 (ppm)
CH2Cl2
C15b
O
O
O

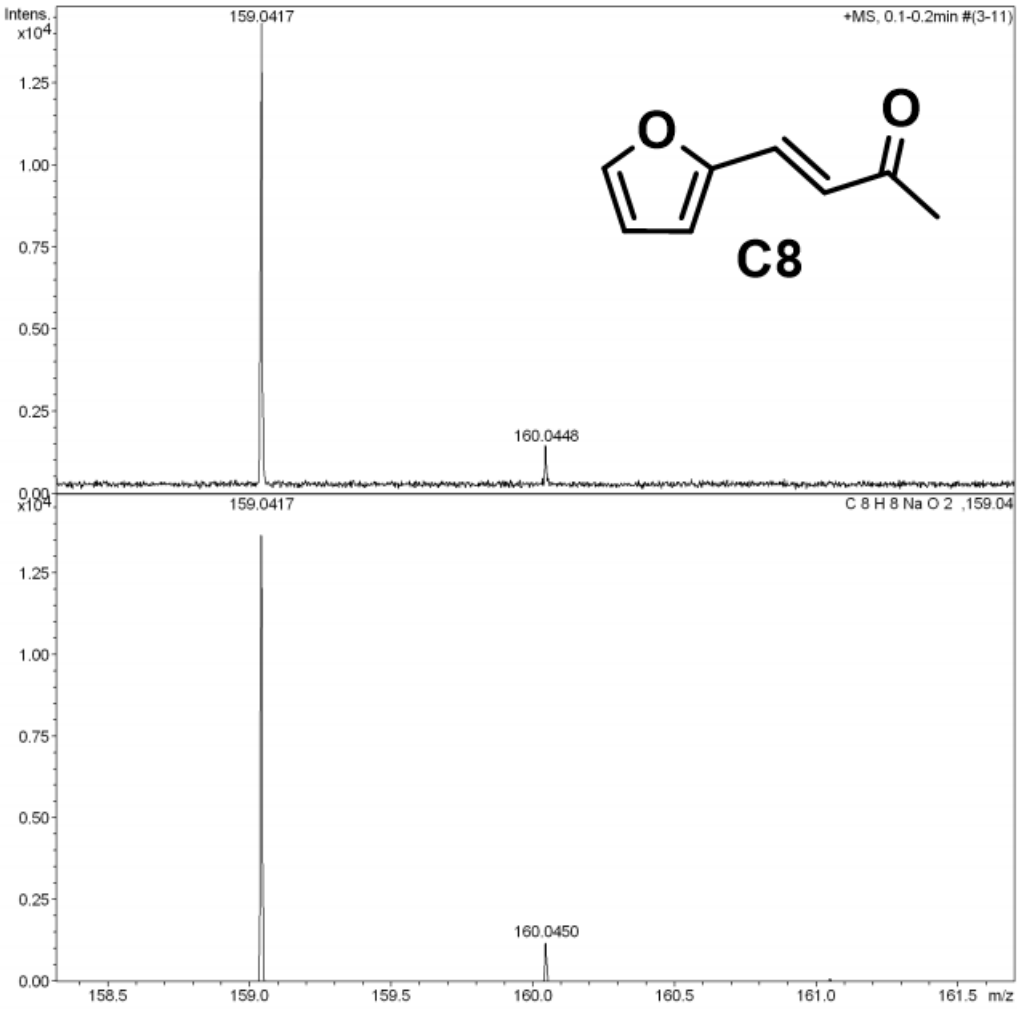
Intens.
x10^4
159.0417
+MS, 0.1-0.2min #(3-11)
1.25
1.00
0.75
0.50
0.25
0.00
160.0448
O
O
C8
159.0417
C 8 H 8 Na O 2 ,159.04
160.0450
158.5
159.0
159.5
160.0
160.5
161.0
161.5
m/z

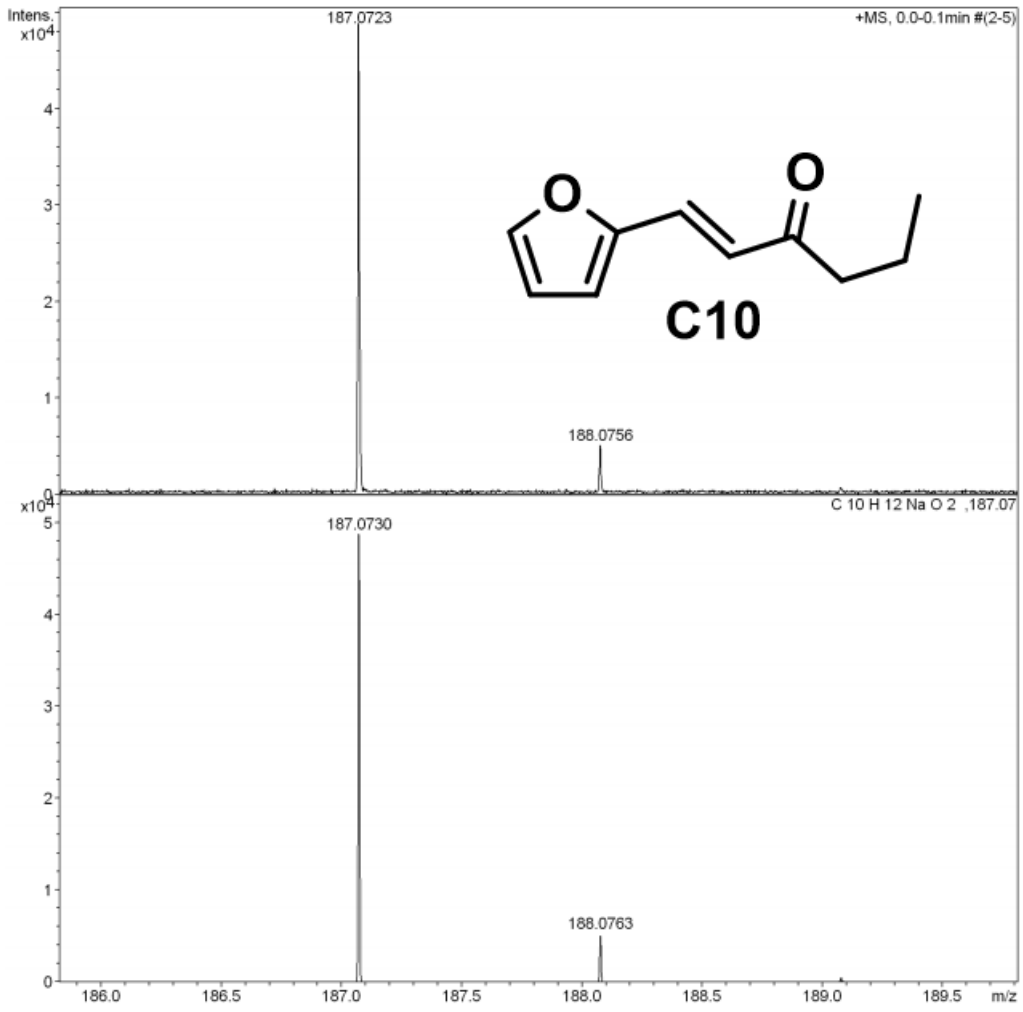
Intens.
x10^4
187.0723
+MS, 0.0-0.1min #(2-5)
O
O
C10
188.0756
C 10 H 12 Na O 2 ,187.07
187.0730
188.0763
186.0
186.5
187.0
187.5
188.0
188.5
189.0
189.5
m/z

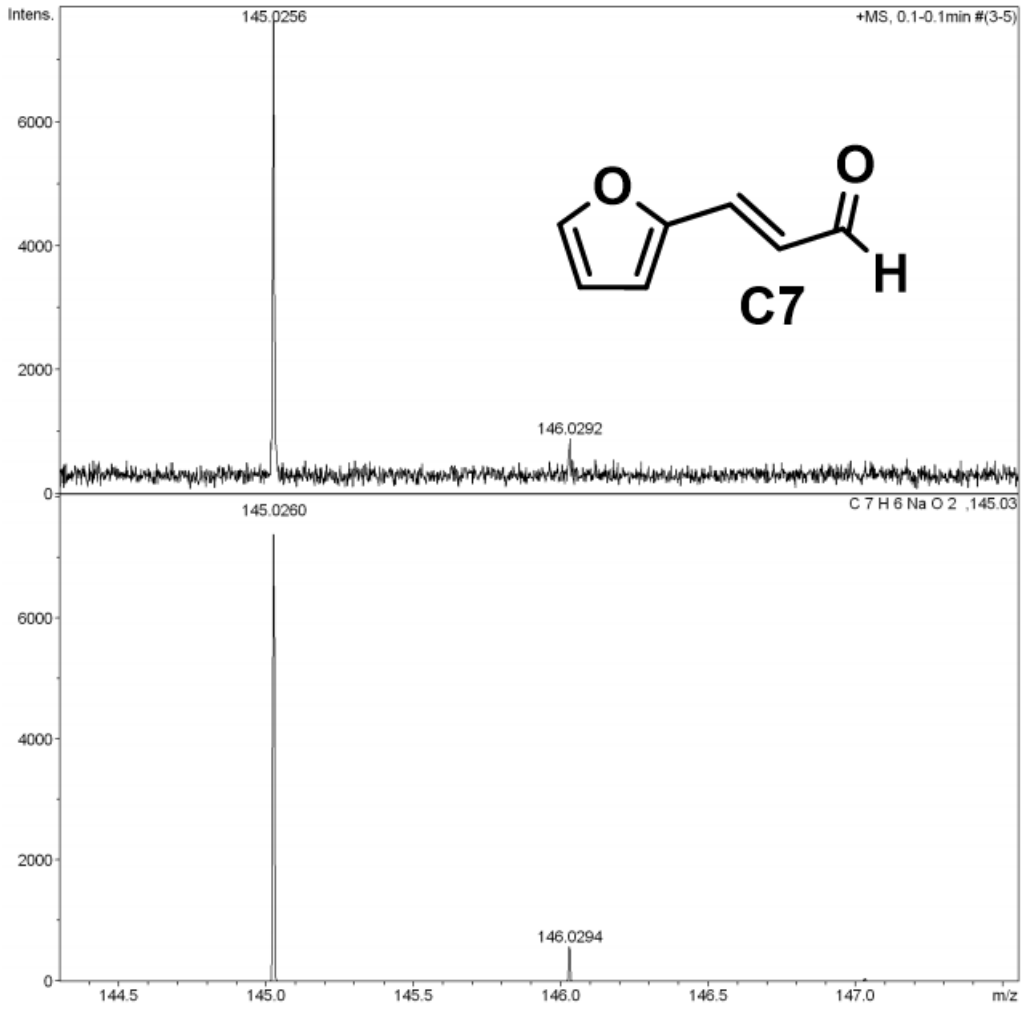
Intens.
145.0256
+MS, 0.1-0.1min #(3-5)
6000
4000
2000
0
O
O
H
C7
146.0292
145.0260
C 7 H 6 Na O 2 ,145.03
6000
4000
2000
0
146.0294
144.5
145.0
145.5
146.0
146.5
147.0
m/z

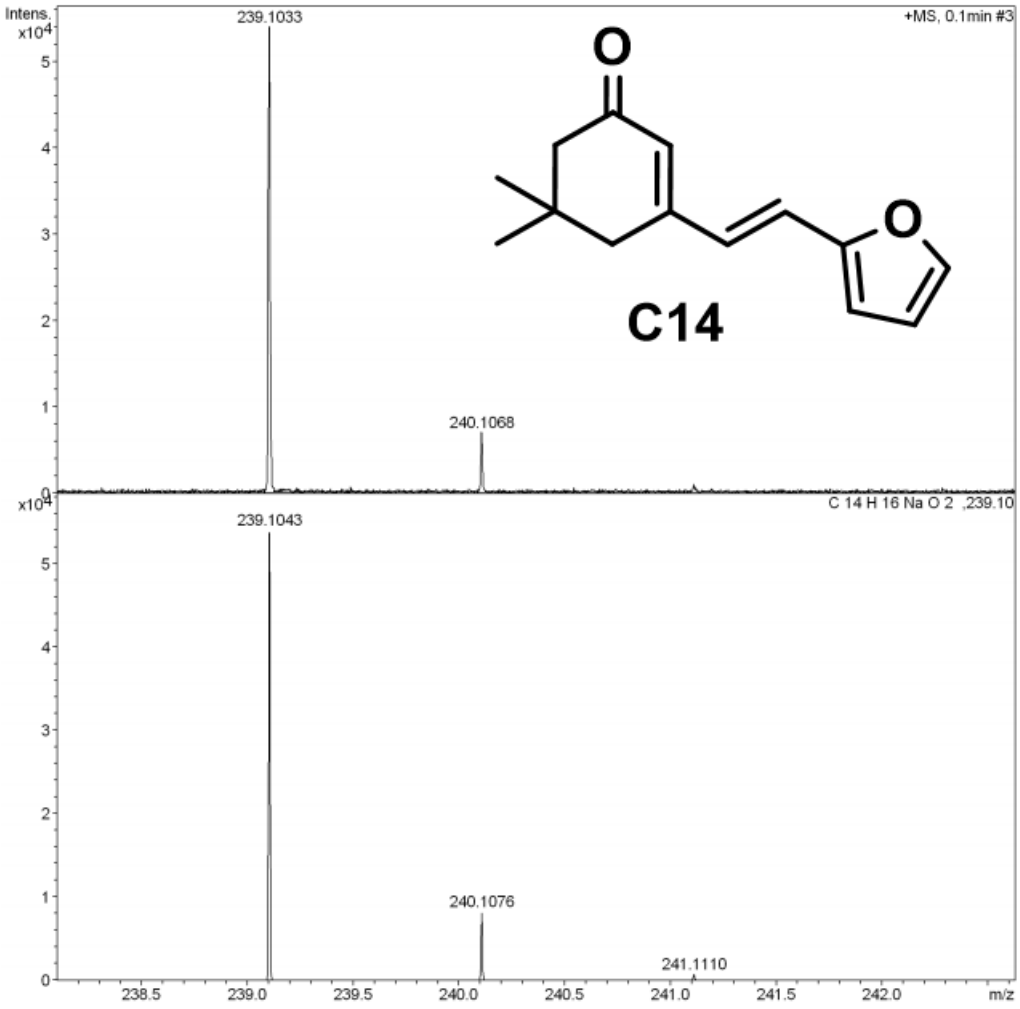
Intens.
x10^4
239.1033
+MS, 0.1min #3
O
O
C14
240.1068
x10^4
C 14 H 16 Na O 2 ,239.10
239.1043
240.1076
241.1110
238.5
239.0
239.5
240.0
240.5
241.0
241.5
242.0
m/z

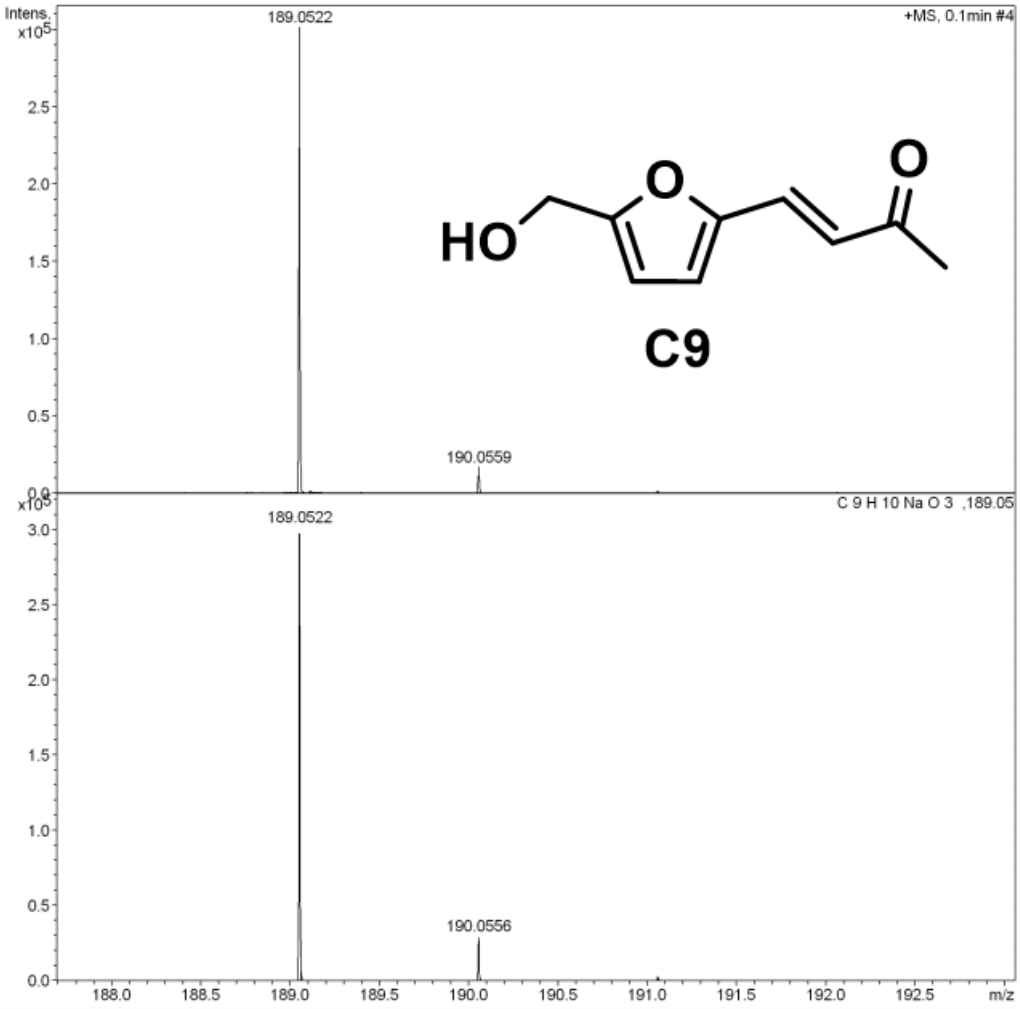
Intens.
x10^5
189.0522
+MS, 0.1min #4
HO
O
O
C9
190.0559
C 9 H 10 Na O 3 ,189.05
189.0522
190.0556
188.0
188.5
189.0
189.5
190.0
190.5
191.0
191.5
192.0
192.5
m/z

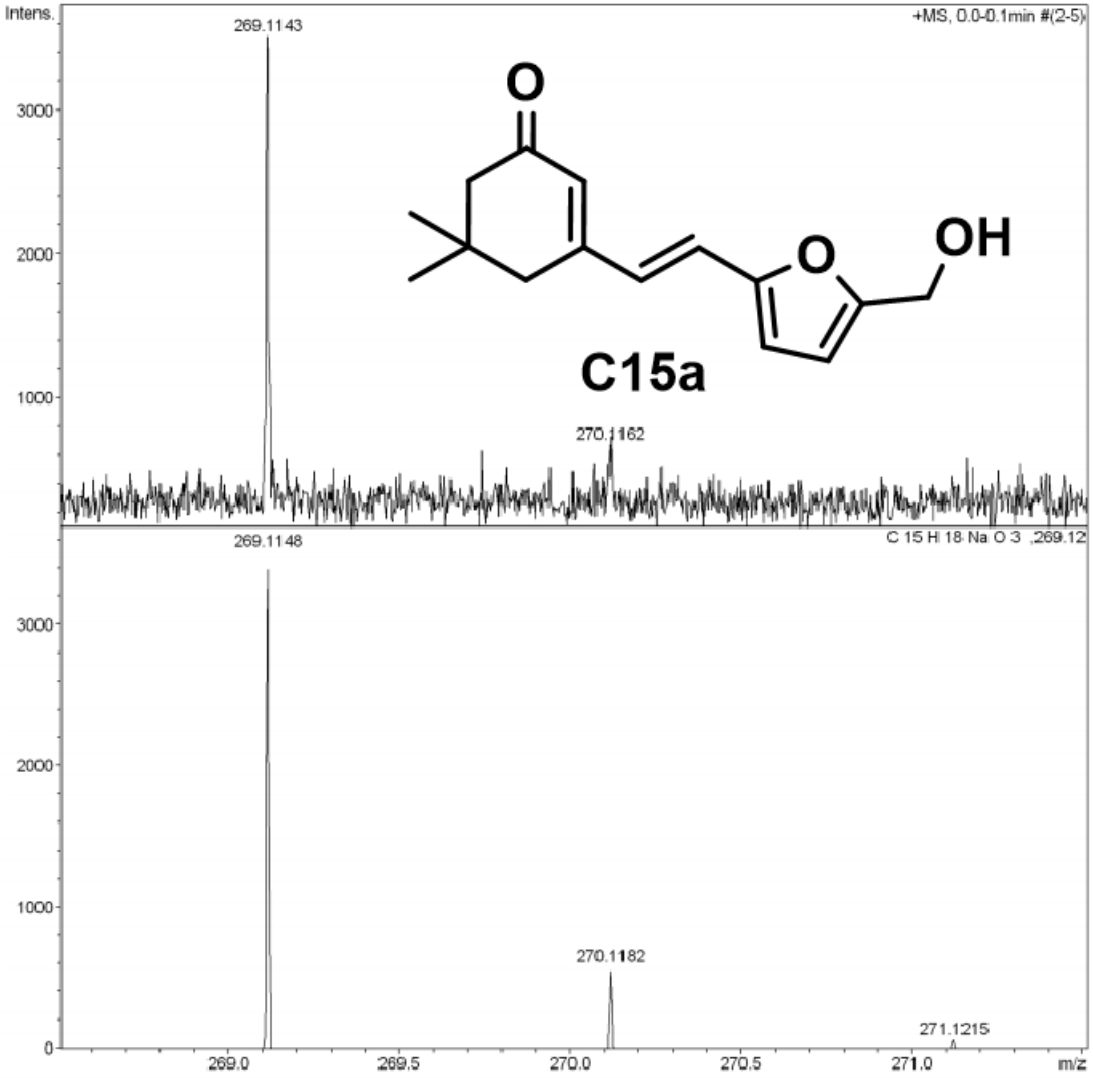
Intens.
+MS, 0.0-0.1min #(2-5)
269.1143
3000
2000
1000
O
O
OH
C15a
270.1162
269.1148
C 15 H 18 Na O 3 ,269.12
3000
2000
1000
0
270.1182
271.1215
269.0
269.5
270.0
270.5
271.0
m/z

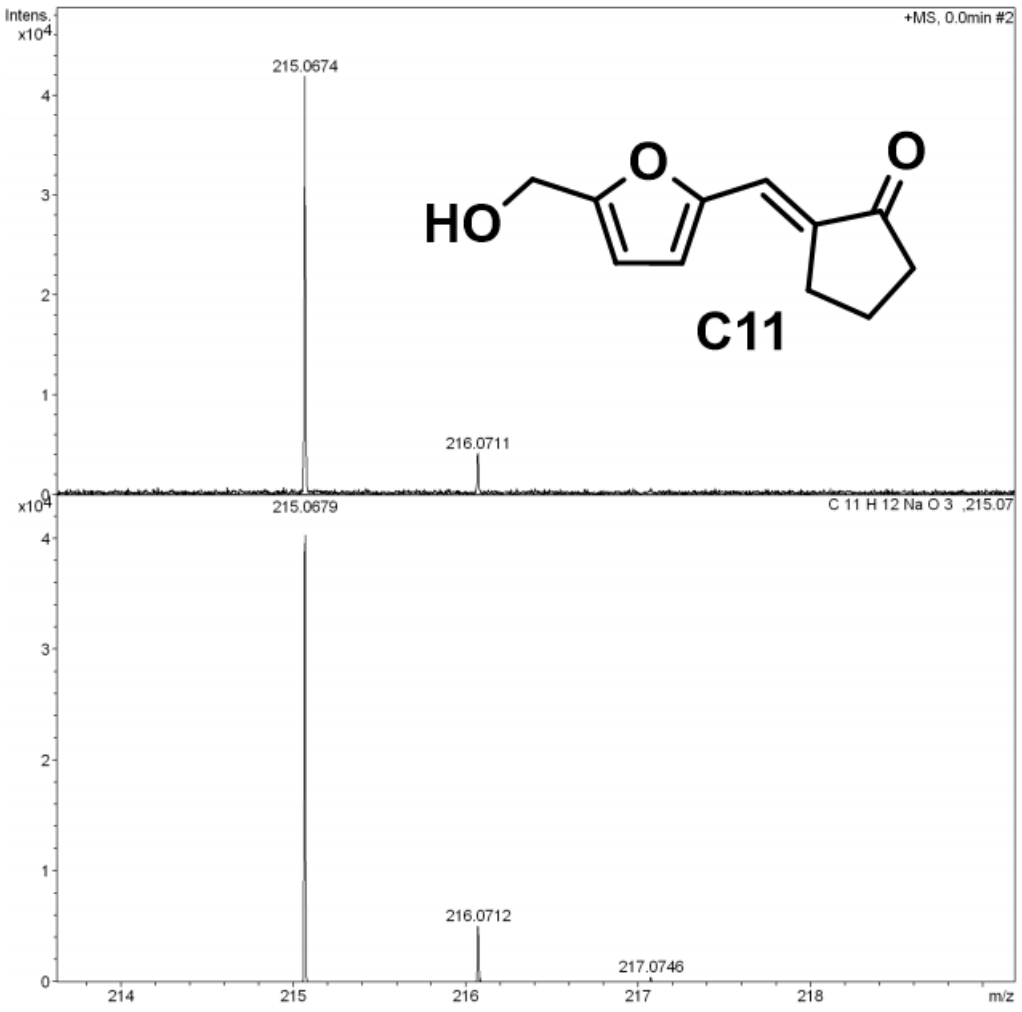
Intens.
x10^4
+MS, 0.0min #2
215.0674
216.0711
HO
O
O
C11
215.0679
C 11 H 12 Na O 3 ,215.07
216.0712
217.0746
214
215
216
217
218
m/z

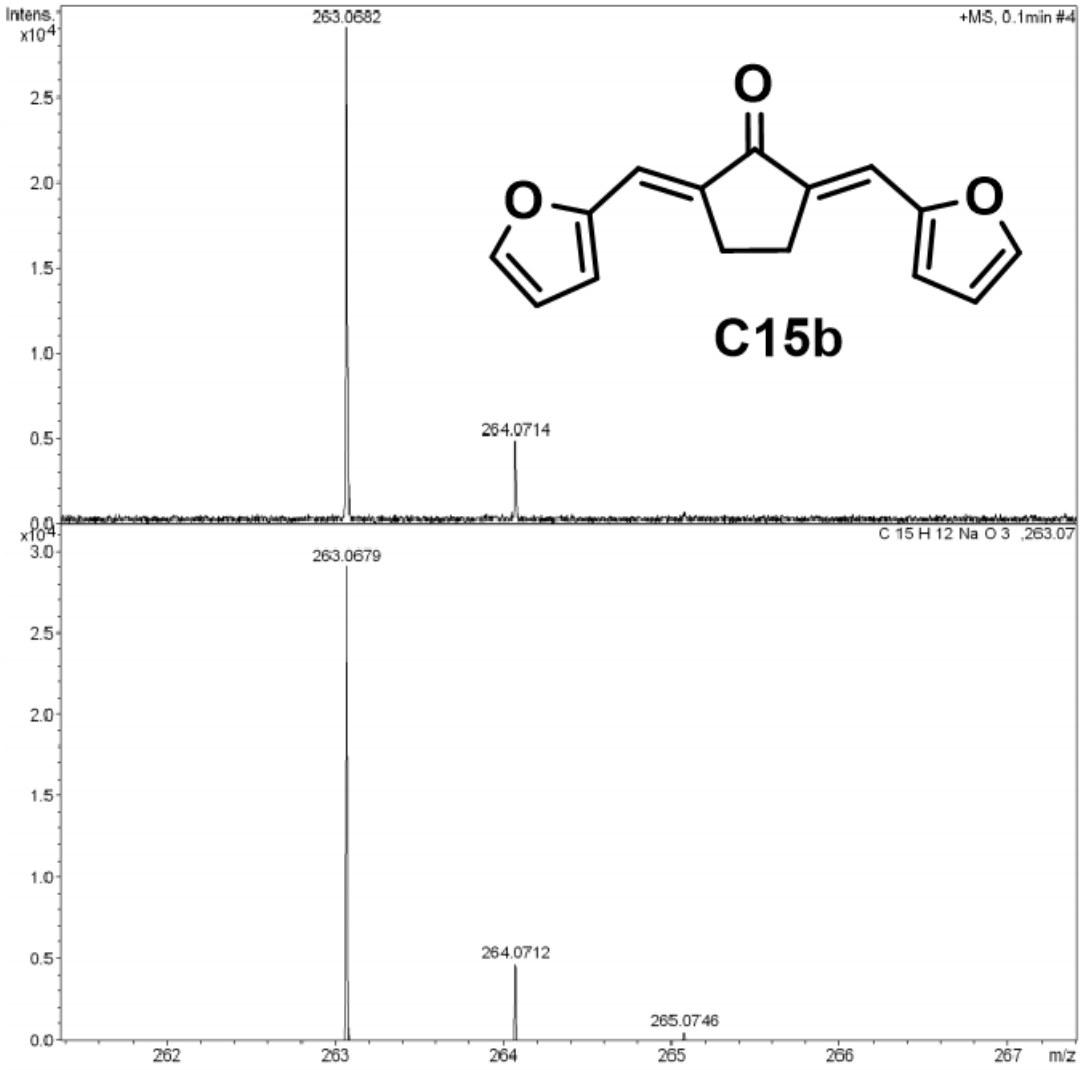
Intens.
x10^4
263.0682
+MS, 0.1min #4
O
O
O
C15b
264.0714
x10^4
C 15 H 12 Na O 3 ,263.07
263.0679
264.0712
265.0746
262
263
264
265
266
267
m/z

4. Supporting References

1. H.-Y. Wang, R. Hu, Y.-J. Lei, Z.-Y. Jia, G.-L. Hu, C.-B. Li and Q. Gu, *Catal. Sci. Technol.*, 2020, **10**, 2821-2829.

2. J. Kou, C. Lu, J. Wang, Y. Chen, Z. Xu and R. S. Varma, *Chem. Rev.*, 2017, **117**, 1445-1514.

3. N. Jin, Y. Sun, W. Shi, P. Wang, Y. Nagaoka, T. Cai, R. Wu, L. Dube, H. N. Nyiera, Y. Liu, T. Mani, X. Wang, J. Zhao and O. Chen, *J. Am. Chem. Soc.*, 2023, **145**, 21886-21896.

4. W. W. Yu, L. Qu, W. Guo and X. Peng, *Chem. Mater.*, 2003, **15**, 2854-2860.

5. I. Lignos, R. M. Maceiczyk, M. V. Kovalenko and S. Stavrakis, *Chem. Mater.*, 2020, **32**, 27-37.

6. J. Premkumar, *Chem. Mater.*, 2004, **16,** 3980-3981.

7. C. Mahala, M. D. Sharma and M. Basu, *Inorg. Chem.*, 2020, **59**, 6988-6999.

8. Y. Hu, X. Q. Hao, Z. W. Cui, J. Zhou, S. Q. Chu, Y. Wang and Z. G. Zou, *Appl. Catal. B Environ.*, 2020, **260**, 118131.

9. Y. Xu and M. A. A. Schoonen, *Am. Mineral.*, 2000, **85**, 543-556.